

The Current Status and Future Directions on Nanoparticles for Tumor Molecular Imaging

Caiyun Yin ^{1,2,*}, Peiyun Hu^{1,2,*}, Lijing Qin², Zhicheng Wang², Hongguang Zhao¹

¹Department of Nuclear Medicine, The First Hospital of Jilin University, Changchun, People's Republic of China; ²National Health Commission (NHC) Key laboratory of Radiobiology, School of Public Health, Jilin University, Changchun, People's Republic of China

*These authors contributed equally to this work

Correspondence: Zhicheng Wang; Hongguang Zhao, Email zhicheng@jlu.edu.cn; zhaohg@jlu.edu.cn

Abstract: Molecular imaging is an advanced technology that utilizes specific probes or markers in conjunction with cutting-edge imaging techniques to observe and analyze the localization, distribution, activity, and interactions of biomolecules within living organisms. Tumor molecular imaging, by enabling the visualization and quantification of molecular characteristics of tumor cells, facilitates a deeper and more comprehensive understanding of tumors, providing valuable insights for early diagnosis, treatment monitoring, and cancer biology research. However, the image quality of molecular imaging still requires improvement, and nanotechnology has significantly propelled the advancement of molecular imaging. Currently, nanoparticle-based tumor molecular imaging technologies encompass radionuclide imaging, fluorescence imaging, magnetic resonance imaging, ultrasound imaging, photoacoustic imaging, and multimodal imaging, among others. As our understanding of the tumor microenvironment deepens, the design of nanoparticle probes for tumor molecular imaging has also evolved, offering new perspectives and expanding the applications of tumor molecular imaging. Beyond diagnostics, there is a marked trend towards integrated diagnosis and therapy, with image-guided treatment playing a pivotal role. This includes image-guided surgery, photodynamic therapy, and chemodynamic therapy. Despite continuous advancements and innovative developments in molecular imaging, many of these remain in the experimental stage and require breakthroughs before they can be fully integrated into clinical practice.

Keywords: molecular imaging, nanoparticles, tumor, diagnosis, treatment

Introduction

Presently, cancer emerges as a paramount challenge in public health, demanding concerted efforts to address its multifaceted complexities. Early detection remains elusive, compounded by its formidable invasive potential and propensity for metastasis, ultimately leading to substantial patient morbidity and mortality. In fact, cancer ranks among the primary contributors to global mortality. Recent statistics have highlighted the severity of this issue, with approximately 19.3 million new cases and nearly 10 million cancer-related deaths worldwide recorded in 2020.¹ Medical imaging technologies are employed to assess tumor, yet the imaging characteristics are primarily represented through subjective, qualitative evaluations. However, factors such as the internal composition of the tumor and inflammatory hyperplasia of lymph nodes can influence this assessment process and are often limited by the individual's imaging interpretation skills. Therefore, enhancing the objectivity and reproducibility of imaging techniques to comprehensively quantify the internal state of tumors could elucidate imaging features that reflect underlying biological changes. Molecular imaging offers the potential for a more thorough understanding of tumors. These methodologies afford insights into the biological underpinnings, pathological manifestations, and growth dynamics of tumors, thereby guiding pivotal aspects of diagnosis, therapeutic intervention, and ongoing monitoring. By precisely delineating the spatial dimensions, staging, and treatment response of tumors, molecular imaging equips healthcare practitioners with invaluable guidance, facilitating informed decisions regarding treatment modalities and the evaluation of therapeutic efficacy.

Moreover, molecular imaging assumes a pivotal role in surgical planning, prognostic evaluation, and the formulation of personalized therapeutic regimens, thus optimizing patient outcomes through tailored interventions.

Molecular imaging represents a sophisticated realm within medical imaging, enabling the visualization of molecular and cellular processes at a sub-anatomic level. However, its scope transcends mere anatomical depiction, delving into the intricate biochemical cascades and target-specific localization patterns that underpin disease progression.² Molecular imaging was initially introduced in nuclear medicine, and with technological advancements, its imaging modalities have continuously expanded. These include radionuclide imaging, fluorescence imaging (FI), magnetic resonance imaging (MRI), ultrasound imaging (UI), photoacoustic imaging (PAI), and multimodal approaches that amalgamate distinct imaging modalities. This burgeoning discipline holds promise in furnishing personalized, noninvasive insights into both molecular and anatomical facets of systemic or organ-specific pathologies, leveraging hybrid technologies to achieve this end.³

Molecular imaging still faces numerous challenges. Mastering and advancing the labeling techniques for molecular imaging probes remains difficult. To meet the increasing demands in medical imaging, the development of molecular imaging probes has primarily focused on improving signal-to-noise ratios and enhancing targeting capabilities. Probes based on nanomaterials have demonstrated promising imaging potential and have garnered significant attention. Within the realm of molecular imaging, nanotechnology and its derivative, nanoparticles (NPs), emerge as disruptive innovations, poised to revolutionize diagnostic paradigms.⁴ NPs, owing to their robust and enduring signaling properties, high payload capacity, multimodal imaging capabilities, and precise target-binding affinities facilitated by multifunctional ligands, constitute a versatile toolkit for molecular imaging applications. Diverse typologies of NPs, distinguished by size, morphology, and material composition, have been conceptualized to cater to distinct diagnostic imperatives. Some classifications distinguish between organic and inorganic NPs; the first group includes dendrimers, liposomes, polymeric NPs and so on, while the latter includes fullerenes, quantum dots (QDs), gold NPs and so on, and others are classified based on whether NPs are carbon-based, ceramic, semiconductor, or polymer.⁵ Enhancing biosensing and improving imaging capabilities can be achieved by modifying the structure of NPs and incorporating other NPs.^{6,7} Functionally, therapeutic NPs serve a dual role, concurrently serving as diagnostic agents to delineate disease localization, subtype, and treatment response, while also facilitating therapeutic interventions through targeted drug delivery or intraoperative guidance for tumor resection.⁸

In the following discussion, we will concentrate on the particular pairing of NPs and molecular imaging, their applications in cancer, and the latest trends in tumor molecular imaging.

The Novel Techniques and Methodologies Based on Nanoparticles for Tumor Molecular Imaging

With their diminutive scale, NPs exhibit an array of unique physical, chemical, and biological characteristics, rendering them adaptable to a multitude of imaging modalities. Herein, we succinctly expound upon frequently utilized NPs across diverse imaging techniques, elucidating their distinctive attributes, as is shown in [Table 1](#). Through the modulation of NP surface properties or structure, bespoke imaging capabilities are engendered, thereby enhancing contrast and resolution in images, and potentially transcending conventional imaging modalities. Deliberate design facilitates NPs to selectively interface with specific cells or tissues, notably tumor cells, thereby amplifying targeting efficacy and yielding pivotal insights into tumor diagnosis. Furthermore, adherence to stringent biocompatibility criteria underscores the extensive applicability of NPs, portending promising prospects in the realm of biomedical imaging. Certainly, different imaging techniques possess distinct characteristics ([Figure 1](#)). Next, we will focus on novel techniques and methodologies to describe research in tumors.

Radionuclide Imaging

Nuclear medicine utilizes radioactive isotopes to diagnose and treat medical conditions, such as by using imaging techniques with radioactive isotopes to observe the organs and tissues inside the human body. Nanotechnology offers the potential for heightened control and precision in this domain, thereby augmenting the accuracy and efficacy of

Table I Nanoparticles Used in Different Imaging Techniques and Their Characteristics

Imaging technique	Nanoparticles	Properties	References
Radionuclide imaging	Liposomes	Biocompatibility, stability, ease to synthesize, high drug loading efficiency, high bioavailability	[9]
	Organic polymer	Synthetic versatility	[10]
	Metal oxide nanoparticles	Ultrafine size, magnetic, biocompatibility	[11–13]
	Nanoemulsions	Kinetically stable	[14]
	Bimetallic nanoparticles	Beneficial electrocatalytic, magnetic, electrical properties	[15]
	Metallic nanoparticles	Inert, biocompatible, low toxicity	[16–18]
Fluorescence imaging	Metallic nanoparticles	Small molecular size, hydrophilicity	[19]
	Organic polymer nanoparticles	High absolute quantum yield, excellent photothermal conversion efficiency, high molar absorption coefficient, high signal-to-noise ratio	[20–23]
	Quantum dots	Easy surface functionalization, photostable, water-soluble	[24–26]
Magnetic resonance imaging	Doped carbon dots	Low toxicity, physicochemical, photostability, excellent biocompatibility	[27]
	Metallic nanoparticles	Large surface area, fast exchange of relaxed water molecules	[28]
	Metal sulfide nanoparticles	Excellent biocompatibility, good photothermal conversion efficiency	[29]
	Composites nanomaterials	Good biocompatibility, safety.	[30]
	Metal-organic frameworks	Large surface area, high porosity, tunable structures	[31]
	Bioresponsive Nano-Sized Contrast Agents	Exhibiting excellent UHF magnetic resonance capability	[32,33]
Ultrasound imaging	Nanobubbles	High stability, longevity and high surface area per volume	[34,35]
	Gas vesicles	Excellent ultrasound contrast signal, high tumor penetration ability	[36]
	Nanodroplets	Faster resolution, longer circulation time, effective tumor vascular permeability	[37,38]
Photoacoustic imaging	Metallic nanoparticles	Strong extinction coefficient, shape dependent optical properties	[39–41]
	Polymeric semiconductor nanoparticles	Excellent photostability, biocompatibility	[42,43,118]

radioactive isotope imaging. Through the integration of nanotechnology, radioactive isotopes can be precisely directed to lesion sites, facilitating more refined diagnosis and treatment. Nanocarriers play a pivotal role in aiding radioactive isotopes to traverse biological barriers, thereby enabling their targeted delivery to tissues or cells, consequently enhancing imaging sensitivity and resolution. Additionally, the application of nanomaterials can mitigate harm to healthy tissues, thereby bolstering the safety and efficacy of treatment.

When designing imaging agents, careful consideration must be given to the selection of radioactive isotopes based on the imaging technique employed. β^+ and γ emitters are considered perfect radioactive isotopes for imaging inside the body. Commonly used isotopes for Single Photon Emission Computed Tomography (SPECT) imaging include ^{99m}Tc , ^{111}In , and ^{188}Re .⁴⁵ For Positron Emission Tomography (PET) imaging, isotopes such as ^{64}Cu , ^{124}I , and ^{18}F can be utilized for labeling.⁴⁶ Radioactive isotopes can either be encapsulated within NPs, serve as the primary constituents of

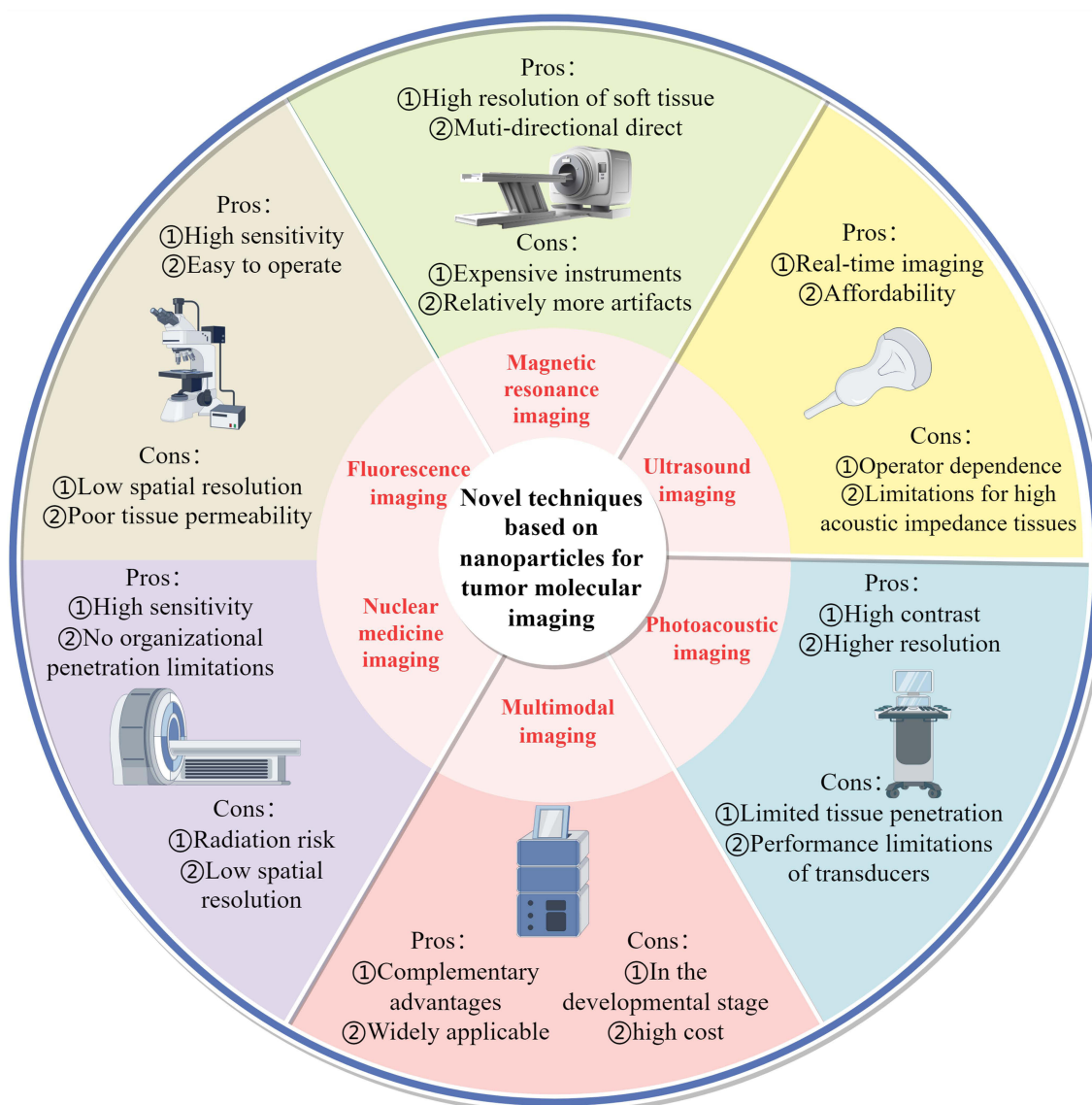


Figure 1 Novel Techniques Based on Nanoparticles for Tumor Molecular Imaging (By Figdraw 2.0). The figure illustrates nanoparticle-based molecular imaging techniques for tumors, along with their respective advantages and disadvantages.

NPs, or be conjugated directly or via chelating agents onto their surfaces. Radioactive isotopes incorporated within NPs can be targeted to tumors using passive or active targeting strategies. Liposomes containing radioactive isotopes have been employed in studies focusing on biodistribution, pharmacokinetics, and targeting. For instance, research has demonstrated that liposomes labeled with ^{111}In , conjugated with cyclic RGDfK, effectively achieve in vivo SPECT imaging and targeted delivery to tumors.⁹ Organic polymer NPs, due to their synthetic versatility, represent optimal platforms for the creation of multifunctional theranostic nanosystems. In a recent advancement, a star-shaped copolymer with 7–8 center-cross-linked arms was synthesized. By modifying multiple arms, researchers aimed to create radiolabeled multifunctional nanoprobe.¹⁰

The spatial resolution of radioactive isotope imaging is limited. Iron oxide (IO) NPs possess inherent magnetic properties, and when labeled with radionuclides, they facilitate the integration of high-sensitivity SPECT or PET with high-spatial-resolution MRI.⁴⁷ Jang HM et al have developed Cu-64-doped IO NPs without chelating agents, suitable for PET-MRI. The ^{64}Cu doping at the core of the core-shell structured IO NPs exhibits excellent in vivo stability.¹¹ NPs of nonradioactive elements with high atomic numbers exhibit strong absorption of X-rays, serving both as contrast agents

(CAs) for radiographic imaging and as sensitizers for radiotherapy. Recent studies have demonstrated that ^{99m}Tc -labeled natural compound nanoemulsions and dual gold-silver NPs labeled with ^{68}Al synthesized using tryptophan can be employed for imaging and biodistribution of breast cancer. ^{131}I labeled polyethylenimine (PEI) captures gold NPs functioning as an innovative nano-probe for SPECT/CT imaging and radioisotope therapy, targeting tumors that over-express Matrix Metalloproteinase 2 (MMP 2). Polyethylene glycol (PEG)-coated gold NPs labeled with ^{211}Pb can be utilized for α particle therapy in pancreatic cancer and glioblastoma. Fourth-generation polyamidoamine dendrimers decorated with neuropeptides and folate, internally embedded with gold and labeled with ^{177}Lu , are effective for imaging and treatment of lung cancer. Silver NPs labeled with ^{131}I , synthesized using turmeric as a reducing and coating agent, can also be used for lung cancer imaging. Additionally, a novel biodegradable polymer microsphere capable of loading ^{177}Lu and MgO NPs can be used for interventional radioembolization therapy in liver cancer and real-time SPECT imaging.^{12,14–18}

Nanotechnology holds promise for enhancing the imaging efficacy of radioactive isotopes in diagnosis and treatment monitoring. Rainone et al conducted a study showcasing the utilization of trastuzumab half-chain conjugated, doxorubicin (DOX)-encapsulated, and ^{99m}Tc radiolabeled silica NPs for targeted SPECT imaging and therapy of HER2-overexpressing breast cancer. Examination of the effectiveness of treatment using PET imaging in vivo demonstrated a notable decrease in tumor size compared to conventional drugs, indicating higher efficacy of this silica-based nanomedicine.⁴⁸ Recently, Wu et al developed polyethylene glycol-poly(lactic acid) (PEG-PLA) NPs incorporating chemotherapy drug 5-fluorouracil (5-FU) and therapeutic radiopharmaceutical ^{131}I . Functionalization of NPs with tumor-targeting antibody cetuximab demonstrated targeted delivery, apoptosis induction, and combined therapy effects in colorectal cancer cells.⁴⁹

It is noteworthy that there exists an intriguing phenomenon in radionuclides, especially those that emit β particles, known as Cherenkov radiation (CR). This refers to the continuous blue light emission resulting from the interaction between charged particles moving faster than the speed of light and dielectric materials.⁵¹ CR can induce the excitation of optical probes in deep tissues through the Cherenkov radiation energy transfer (CRET) process, enabling imaging of deep-seated tissues. Additionally, the targeted CR of radioactive tracers provides internal excitation for photodynamic therapy (PDT), offering new avenues for tumor diagnosis and treatment. For instance, researchers have designed a nano-composite material comprising ^{89}Zr - TiO_2 - MnO_2 , utilizing CR generated from the interaction of ^{89}Zr with surface NPs to activate TiO_2 and MnO_2 for reactive oxygen species (ROS) production, thereby promoting tumor therapy. Simultaneously, ^{89}Zr serves as a PET imaging agent, providing visualization information for the NP delivery.¹³ Guo R et al demonstrate that extracellular vesicles derived from goat milk can serve as carriers to deliver the photosensitizer Chlorin e6 (Ce6), while tumor-avid ^{18}F -FDG can activate Ce6-induced therapy for tumors.⁵² Furthermore, some researchers have utilized ^{68}Ga radiopharmaceuticals as in-situ excitation sources.⁵³ Notably, they have innovated the fluorescent probes by exploiting the narrow emission bands of lanthanide element Europium (Eu) complexes in the visible and NIR (near-infrared) regions to optimize the probe performance. Experimental findings conducted in living organisms show that the in-situ excitation of Eu (III) emission by ^{68}Ga leads to a fivefold amplification of the optical signal, thus enabling the removal of tumor tissue. In conclusion, the integration with nanomedicine can significantly expand the scope of nuclear medicine, providing unique advantages in terms of sensitivity and specificity in diagnosis/treatment, imaging resolution, and scalability.⁵⁰

Fluorescence Imaging

FI necessitates an external light source, such as a lamp, laser, or LED, to excite fluorescent substances. Subsequently, the emitted fluorescence is detected using an optical imaging system. Compared to traditional MRI and CT techniques, FI offers advantages such as super spatial resolution, immediate image capture, and cost-effectiveness.^{54–58} Near-infrared fluorescence (NIRF) probes have garnered significant attention in the field of organic small-molecule fluorescent sensors due to their superior optical tissue penetration, minimal impact to biological samples, and low background noise, bringing them closer to clinical applications.⁵⁹

The core structure of fluorescent molecular probes is the fluorophore. Indocyanine green (ICG), a sulfonated cyanine dye centered around Cy7.5, has emerged as the sole NIRF dye sanctioned by the US Food and Drug Administration

(FDA) for clinical diagnostics due to its excellent safety profile.⁶⁰ Beyond cyanines, other fluorescent groups such as squaraines, rhodamines, BODIPY, and Dicyanoisophorone are also under active investigation.^{61–64}

Fluorescent NPs frequently integrate nanotechnology with fluorescent dyes, offering optimized photon quantum yield and photostability compared to conventional dyes due to their facile surface modification and tunable particle size.⁶⁵ Despite advancements in accumulation via the enhanced permeability and retention effect and active targeting strategies, these probes are often limited by high background noise and false-positive signals due to their persistent “on” state.⁶⁶ Activatable probes, dormant in surrounding tissues but selectively triggered at tumor sites, represent a promising approach for improved imaging. Generally, fluorescent molecular probes exhibit weak or negligible fluorescence in their inactive state; however, under specific conditions, such as the presence of particular chemicals or biological processes, they undergo significant changes in fluorescence properties, leading to a strong signal and high signal-to-background ratio (SBR). Fluorescence restoration and quenching have been achieved through various mechanisms, including Förster resonance energy transfer (FRET) (Figure 2A), photoinduced electron transfer (PeT) (Figure 2B), aggregation-induced emission (AIE) (Figure 2C) and so on.⁶⁷

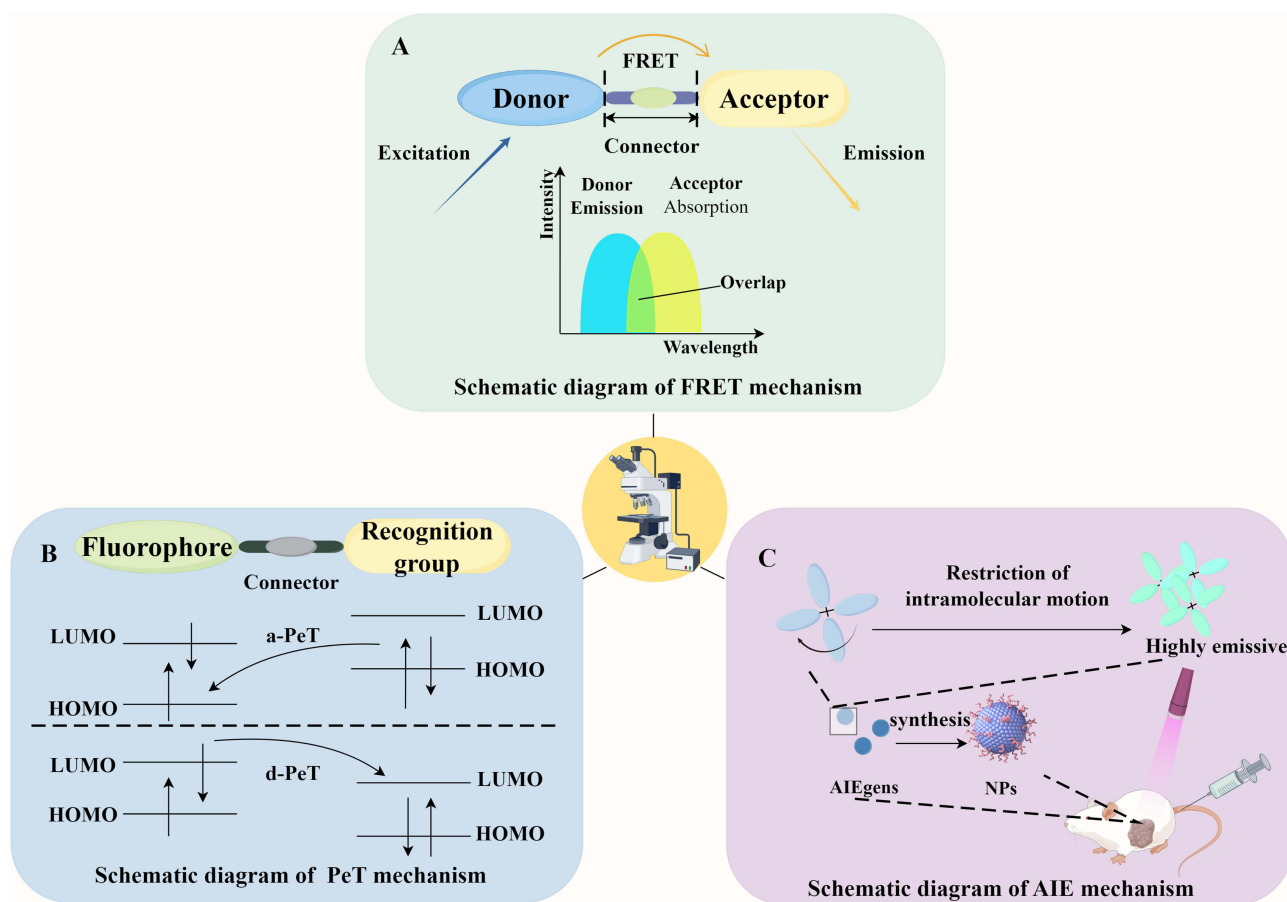


Figure 2 Schematic Diagram of the Design Principles of Activatable Fluorescent Probes (By Figdraw 2.0). As shown in the figure, the design principle of the activatable probes is illustrated. **(A)** illustrates the mechanism of FRET. In this process, when the energy acceptor and donor are in close proximity, the donor in its excited state transfers some of its energy non-radiatively to the acceptor. This energy transfer causes the acceptor to become excited and emit fluorescence, while the donor's own fluorescence is quenched. **(B)** depicts the mechanism of PeT, which can be categorized into acceptor-excited (a-PeT) and donor-excited (d-PeT) mechanisms. In a-PeT, the highest occupied molecular orbital (HOMO) energy level of the recognition group is positioned between the HOMO of the fluorophore and its lowest unoccupied molecular orbital (LUMO) energy level. Consequently, electrons from the HOMO of the recognition group can be transferred to the HOMO of the excited-state fluorophore. This prevents the electrons in the LUMO of the fluorophore from returning to the ground state, leading to fluorescence quenching. In d-PeT, the LUMO of the recognition group lies between the HOMO and LUMO energy levels of the fluorophore. Upon excitation of the fluorophore, electrons are transferred from its HOMO to its LUMO and then non-radiatively jump into the empty LUMO of the recognition group, leading to fluorescence quenching. **(C)** demonstrates the mechanism of AIE. AIEgens, which have a specific molecular structure, experience restricted intramolecular motion upon aggregation. This restriction causes the release of energy in the form of radiative transitions, resulting in significantly enhanced luminescence.

FRET occurs when the emission spectrum of a donor molecule (fluorescent probe) overlaps with the excitation spectrum of a receptor molecule (another fluorophore). The donor's fluorescence leads to the receptor's fluorescence, reducing the donor's intensity. The extent of FRET is intricately linked to the physical separation between the donor and acceptor molecules. A common design strategy involves anchoring the donor-receptor pair in close proximity within the same system or molecule, introducing reaction units as specific recognition groups, and ultimately constructing a FRET system. When exposed to specific target analytes, the FRET process is initiated or inhibited, and changes in fluorescence signal indicate the presence of the analytes. Liu J et al developed a nanoscale probe termed D/I-PNT for NIR-I biological imaging to detect endogenous methylglyoxal induced by glyoxalase 1 inhibitors in a 4T1 tumor-bearing mouse model using FRET.²⁰

PeT is another mechanism for designing activatable nanoprobe, involving electron transfer within or between molecules under light-induced conditions. When the probe molecule is illuminated, electrons transfer from the donor to the excited-state fluorophore, resulting in either non-emission or weak emission from the donor molecule. Upon binding with the analyte, PeT is hindered, restoring the fluorescence emission of the fluorescent substance.⁶⁸ Yan R et al devised an enzyme-responsive, in-situ self-assembling nanoscale probe (P-CyFF-Gd) for real-time NIR FI. Alkaline phosphatase (ALP) recognizes the phosphate groups (-PO₃H) appended to the NIR fluorophore (merocyanine, Cy-Cl), inducing a PeT effect that ultimately leads to quenching. Upon interaction with ALP, the -PO₃H groups are cleaved from P-Cyff-Gd, restoring fluorescence. Simultaneously, owing to the presence of hydrophobic dipeptides (Phe-Phe (FF)), the self-assembled NPs remain localized on the cell membranes (CMs) to demonstrate ALP activity and localization. The retention time in tumor tissue can be extended by the accumulation within the CM or lysosomes, consequently improving the contrast of NIR FI.¹⁹

AIE can also achieve similar purpose. Traditional organic fluorescent dyes typically exhibit strong emission when dispersed, but fluorescence diminishes or is quenched in aggregated states at high concentrations, a phenomenon known as aggregation-caused quenching.⁶⁹ In contrast, AIE represents the opposite phenomenon, where AIE probes emit fluorescence when aggregated or when molecular rotation is restricted. Xu L et al initially developed and synthesized the NIR aggregation-induced emission luminogen (AIEgen) QM-TPA-Gal. In *in vivo* experiments using an ovarian tumor model, the hydrophilic and non-fluorescent QM-TPA-Gal, upon entering cells, is hydrolyzed by β -Gal to produce hydrophobic QM-TPA-OHs. These then aggregate into NPs, "activating" NIRF through the AIE mechanism. This process exhibits exceptional sensitivity, specificity, and biocompatibility.²¹ In addition, different functional groups respond differently to the environment. By incorporating them into the AIE framework, the properties of AIEgens can be influenced to achieve activation purposes.⁷⁰ AIEgens exhibit strong fluorescence in aggregated states, providing significant advantages for detecting minute residual tumors in the tumor bed and metastatic lymph nodes.²² However, most AIEgens are hydrophobic. Encapsulating AIEgens into polymer NPs is an effective method to improve their water dispersibility and biocompatibility. Some researchers have encapsulated AIEgens in optimized protein nanocages, achieving targeted FI of tumors and mitochondria in *in vivo* experiments.⁷¹

A good fluorescent probe should possess excellent fluorescence stability, characterized by strong photobleaching resistance, pH stability, a long fluorescence lifetime, and a high quantum yield. QDs, which are semiconductor nanocrystals capable of emitting fluorescence, have emerged as an innovative form of fluorescent labeling material. These materials offer distinct benefits for extending the observation of biological processes and tracking activities within living organisms. Compared to traditional organic fluorescent reagents, QDs boast numerous advantages, such as narrower fluorescence spectra, higher quantum yields, greater photochemical stability, and resistance to decomposition. Recently, several new QDs have been developed and utilized in fluorescence imaging.²⁴⁻²⁶ It is worth noting that it has important potential value. Carbon quantum dots exhibit favorable fluorescent properties, and their performance can be optimized through surface structure modification and heteroatom doping to achieve fluorescence enhancement, making them suitable for biosensing and imaging applications.^{6,7} Some researchers have combined carbon dots with iron-based magnetic NPs, which not only enhance fluorescence but also provide a valuable reference for achieving multimodal imaging.⁷² Ghosh T et al have also doped carbon dots with holmium and manganese ions to create novel nanoprobe for pH sensing and MRI imaging.⁷³ Such probes endow carbon dots with the potential to expand imaging modalities.

Tissue absorption, scattering, and autofluorescence impose limitations on the resolution of *in vivo* FI. In comparison to FI, phosphorescence imaging can alleviate the interference of biological autofluorescence to some extent and achieve higher-quality images and higher signal-to-noise ratios (SNRs) through time-resolved imaging techniques. Organic room-temperature phosphorescence (RTP) materials have been identified as a novel class of afterglow imaging agents, characterized by superior biocompatibility and high SNRs, thus circumventing autofluorescence in *in vivo* imaging.^{74,75} The spread of tumors to the lungs creates a specialized microenvironment, and the early metastatic stage preceding the formation of secondary tumors can be detected using phosphorescence imaging. In the study by Chang K. et al, phosphorescent NPs synthesized from phenothiazine derivatives were utilized in a 4T1 lung metastasis mouse model. Compared to other major organs (including the heart, liver, spleen, and kidneys), only the lungs exhibited bright phosphorescent emission, demonstrating high selectivity for metastatic tumors.²³

Magnetic Resonance Imaging

MRI is an emerging modality for molecular imaging, offering high-resolution three-dimensional imaging to evaluate biological processes within solid tumors, thereby guiding precision healthcare for individuals with cancer. MRI CAs are molecular compounds engineered to modify the magnetic properties of nuclei, particularly proton, thereby enhancing contrast between different regions within an image. Gadolinium-based contrast agents (GBCAs) have found widespread use in both preclinical and clinical settings.^{76,77} Nevertheless, gadolinium (Gd) chelates employed in tumor MRI face obstacles including insufficient sensitivity, absence of specificity, and the potential for Gd leakage.

Nanoscale targeted CAs have shown potential for enhancing contrast specifically in tumors during preclinical investigations. Du J et al synthesized Gd-doped carbon dots (Gd-CDs) through a hydrothermal method and conjugated them with folate molecules to form Gd-CDs-FA, enhancing both FI and MRI capabilities. *In vitro* MRI studies revealed that Gd-CDs-FA had a relaxivity rate of $13.56 \text{ mM}^{-1}\text{s}^{-1}$, surpassing the relaxivity rate of the clinical CA Gd diethylenetriamine pentaacetate (Gd-DTPA), indicating its superior relaxivity. *In vivo* experiments on nude mice showed that, following the injection of Gd-CDs-FA, the microstructure of organs and tissues showed no histological damage or necrosis, confirming their biocompatibility. Additionally, they exhibited targeted MRI of liver cancer, establishing a robust foundation for the targeted MRI diagnosis and monitoring of liver cancer.²⁷ Liu S et al proposed a single-atom Gd nanocontrast agent (Gd-SA) to enhance tumor MRI. The individual Gd atoms were coordinated by six N atoms and two O atoms, distributed on carbon nanospheres with cavities, to optimize the efficiency of Gd atoms utilization and reduce the potential for toxic Gd ion release. *In vivo* MRI findings demonstrated that Gd-SA provided superior spatial resolution and a broader imaging time frame for tumors compared to Gd-DTPA, along with lower hematological, liver, and kidney toxicity.²⁸

Safety considerations are paramount for the clinical application of any CA by regulatory agencies. With concerns raised about the safety of GBCAs due to evidence linking Gd to nephrogenic systemic fibrosis and Gd deposition in the brain,^{78,79} paramagnetic manganese (Mn) complexes are gaining interest in this field due to the superior safety profile of Mn (II) ions compared to exogenous Gd, as well as their favorable intrinsic properties such as high magnetic moments, slow electron spin relaxation, and unstable water exchange.^{80,81} Ma G et al prepared a multifunctional polydopamine (PDA)-coated manganese sulfide (MnS) nanocluster. The polyhydroxyl structure of PDA increases the affinity of water towards pH-responsive MnS nanoclusters by facilitating hydrogen bonding interactions. The spin lattice relaxation rate of MnS nanoclusters exhibited a notable increase following the application of PDA coating, which was conducive to efficient tumor MRI.²⁹ Pan X et al utilized gold nanocages as carriers loaded with the drug 5-FU, encapsulated with a MnO₂ shell, providing a suitable strategy for multimodal imaging to facilitate coordinated therapy.³⁰

IOs have been extensively researched as CAs of MRI due to their uniform size distribution, biocompatibility, and surface functionalization capabilities. The assembly of IOs into larger aggregates enhances R₂ relaxivity, significantly improving T₂-weighted imaging, while the conjugation of various molecules facilitates tumor targeting. Gholipour N et al synthesized biotinylated thiosemicarbazone dextran-coated IOs, which demonstrated enhanced uptake at biotin receptor-positive 4T1 tumor sites.⁸² Qi G et al obtained nanonuclei with excellent magnetic properties and monodispersity through thermal decomposition. Subsequently, the particles were enveloped with a mesoporous silica shell through the Stöber technique, forming a mesoporous material characterized by a substantial drug carrying capacity

and pH sensitivity, crucial for the visualization and targeted DOX release system aimed at pancreatic cancer.⁸³ Beyond IO, other magnetic NPs have garnered significant attention. For instance, FeWO₄, a p-type semiconductor material, exhibits outstanding electronic and optical properties, making it suitable for the development of multifunctional imaging-guided tumor-targeted diagnostic and therapeutic agents.⁸⁴ Besides the use as CAs, Prussian blue NPs, characterized by a peak absorption range of 690–720 nm and a photothermal conversion efficiency of around 20%, function as effective photothermal agents owing to their outstanding ability in converting light into heat energy.⁸⁵ Magnetic metal-organic frameworks (MOFs) combine the advantages of MOF-based drug delivery systems with the inherent magnetic properties of metals, presenting a promising platform for diagnosis and synergistic therapy.⁸⁶ For instance, Fan Y et al developed stimulus-responsive nanoagents, namely ¹⁹F/MOF-TA NPs, utilizing trivalent iron ions and fluorine-containing organic ligands as structural and functional units. These nanoagents were employed for activatable ¹⁹F MRI and synergistic tumor therapy.³¹

Ultra-high field (UHF) MRI is gaining increasing popularity in biomedical research and clinical applications, becoming a focal point in cancer diagnostics. Although current paramagnetic or superparamagnetic MRI CAs can achieve selective tumor signal enhancement in low-field MRI, their efficacy is limited at UHF due to inherent magnetic properties. Liang Z et al reported a magnetic conversion nanoprobe composed of silver-gadolinium bimetallic NPs coated with 3-mercaptopropionic acid (C₃H₆O₂) ligands. This NP features adjustable ligand structures and magnetization intensity, enabling responsiveness to various pH conditions.³² Besides optimizing the structure of CAs, developing new UHF-MRI CAs with high sensitivity is clinically significant. Holmium (Ho), a paramagnetic rare earth element, exhibits an extremely short electronic relaxation time. Under high magnetic field intensity, Ho (III) with an effective magnetic moment of 10.0 μB can induce local magnetic field gradients and shorten transverse relaxation times, making it suitable as high-field T₂ CAs. Zhang R et al synthesized Ho (III)-doped mesoporous polydopamine (Ho-MPDA, HM) containing Mitoxantrone and targeted breast cancer by encapsulating 4T1 CMs. The results revealed significant UHF T₂ MRI characteristics ($r_2=152.13 \text{ mM}^{-1}\text{s}^{-1}$) and a high drug loading capacity of up to 18%. This formulation was used for tumor-targeted drug delivery and UHF MRI-guided chemophotothermal therapy.³³ In addition to Ho, the paramagnetic dysprosium (III) ion (Dy³⁺) exhibits the shortest electronic relaxation time ($\tau_e=0.5 \text{ ps}$) and the most elevated effective magnetic moment ($\mu_{\text{eff}}=10.6 \text{ μB}$) among lanthanide ions. This affects proton relaxivity through a Curie mechanism, predominantly influencing T₂. The influence of Curie relaxation significantly rises with the external magnetic field and is proportional to the lanthanide ion's magnetic moment squared, resulting in notably effective r_2 relaxation in UHF-MRI applications.⁸⁷

Chemical exchange saturation transfer (CEST) MRI represents a potentially valuable molecular imaging modality, capable of specifically detecting metabolites containing exchangeable amide, amine, and hydroxyl protons. CEST CAs need to possess exchangeable proton groups, such as alcohol, amine, amide, and acid groups, which resonate at Larmor frequencies for selective saturation.⁸⁸ Various paramagnetic or superparamagnetic nanoscale CAs have been investigated for applications in cancer phenotyping and neurological diseases, aiming to characterize tumor metabolism features such as hypoxia in tumor cells,⁸⁹ extracellular pH,⁹⁰ specific enzymes in tumor regions,⁹¹ and water exchange levels on CMs.⁹² For instance, Kombala CJ et al pioneered the development of paramagnetic nanoscale polymers for pH measurement using acido CEST MRI. Utilizing 4-aminosalicylic acid ester as a monomer unit facilitated selective saturation, potentially allowing for higher saturation levels and thereby improving detection sensitivity. Additionally, the concentrations used in acido CEST MRI studies were reduced by 125-fold and 488-fold compared to monomeric CAs and iodopamide, respectively.⁹³

Ultrasound Molecular Imaging

The introduction of specific CAs enables molecular UI to achieve highly sensitive detection of particular cells, molecules, or biological processes within the body, offering more precise diagnostic and monitoring information. In recent years, a range of ultrasound contrast agents (UCAs) have been developed to enhance the precision of disease diagnosis in molecular ultrasound cancer imaging.^{94,95} Microbubble CAs are the most commonly utilized in clinical practice, widely employed in routine clinical contrast-enhanced ultrasound (CEUS) imaging examinations.⁹⁶ However, microbubbles cannot extravasate from blood vessels.⁹⁷ In contrast, nano-sized bubbles have the advantage of penetrating blood

vessels and reaching extracellular tissue spaces, especially in tumors. Currently, nanobubbles (NBs), gas vesicles (GVs), and nanodroplet CAs have been developed for the imaging of tumors.⁹⁸ Furthermore, UCAs detect specific disease markers by binding with various targeting ligands.⁹⁹

In recent years, lipid-stabilized NBs with diameters smaller than 1000 nm have become a research hotspot as UCAs. Wang Y et al pioneered the development of a particularly stable NB CA (diameter ranging from 100 to 500 nm) composed of perfluoropropane gas nuclei and stabilized with propylene glycol, phospholipids, and glycerol shells. They equipped NBs with specific antibodies or ligands and, using a more clinically relevant *in vivo* prostate cancer model, conducted UI targeting PSMA.³⁴ With advancements in technology, dual-targeted nano-sized CAs are also continuously being developed. Mi X et al synthesized small-sized NBs (~49 nm) and surface-modified them with alanine-alanine-asparagine (NB-A) or arginine-glycine-aspartic acid peptide (NB-R). These modifications were designed to specifically target lectins present in tumor cells and integrins found in the neovascular system of tumors. Dual-targeted NBs serve as effective UCAs for specific imaging of breast cancer and demonstrate considerable promise for broader applications in cancer diagnosis and surveillance in the future.³⁵

Nanoscale CAs produced through chemical synthesis have been found to exhibit superior acoustic properties, but the majority of these agents have diameters exceeding 500 nm, limiting their penetration capabilities into tumors. Recently, GVVs from halophilic archaea have emerged as promising alternatives to conventional acoustic CAs.³⁶ Nano-bioengineered GVVs derived from *Halobacterium* NRC-1 (Halo) with a diameter of 200 nm have exhibited remarkable ultrasound contrast signals in the livers of mice and enhanced penetration into tumors.^{36,100} Increasing evidence suggests the significant potential of GVVs in UI and therapeutic applications. Abundant evidence indicates a strong correlation between the progression and metastasis of tumors and various extracellular matrix (ECM) proteins. Among these, one of the most abundant ECM components linked to the formation of new blood vessels in tumors is extra domain-B fibronectin (ED-B FN), which is notably increased in numerous highly aggressive cancer types. A cyclic nonapeptide, CTVRTSADC (ZD2), has been developed, exhibiting high specificity for binding to ED-B FN. Feng Y et al first reported an improved acoustic probe based on bioengineered GVVs modified with ZD2 and investigated its potential for early diagnosis of bladder cancer.¹⁰¹ Recently, they isolated GVVs and modified them with LyP-1 peptide (a cyclic nonapeptide ligand specific for targeting p32) and administered the resulting LyP-1-GV system to mice with tumor xenografts, with tumor volumes of 70 mm³ and 1000 mm³ after 7 and 21 days, respectively. Through UI, they demonstrated for the first time the translocation of p32 protein from mitochondria to the plasma membrane, providing a new strategy for exploring molecular events of protein translocation and assessing tumor metastasis at the level of living animals.¹⁰⁰

Nanodroplets typically consist of a perfluorocarbon (PFC) liquid core encapsulated by a lipid shell. They can be stimulated by ultrasound to convert from droplets to gas-filled bubbles. Due to their faster resolution, prolonged circulation time, and efficient tumor vascular permeability, they are being investigated as UCAs.³⁷ Further surface coating or functionalization based on PFC is employed for tumor imaging. For instance, some researchers utilized folate-conjugated liquid perfluorohexane (PFH) as the core of nano-droplets for imaging mouse liver cancer.³⁸ Yang H et al also employed phase-change nano-droplets combined with IR-780 iodide for precise detection of malignant melanoma of the skin.¹⁰² As an effective synergistic delivery system, nanodroplets can be controlled for release through ultrasound. Li J et al assembled targeted nanodroplets for cancer-associated fibroblasts (CAFs), enabling co-delivery for ASCT2 inhibitor and siRNA targeting glutamine synthetase (GLUL). Through ultrasound-targeted microbubble disruption, drugs can be rapidly released, blocking the interaction of CAFs with cancer cells in glutamine metabolism, and downregulating the expression of GLUL. This achieves the dual purpose of CEUS imaging while modulating tumor metabolism.¹⁰³ Additionally, they constructed nanodroplets loaded with simvastatin for comprehensive diagnosis and treatment in a triple-negative breast cancer mouse model.¹⁰⁴

Notably, in recent decades, there has been a growing significance of focused ultrasound (FUS) ablation in the field of biomedicine. Its non-invasive nature provides significant advantages, especially for clinically infeasible surgical interventions.¹⁰⁵ Nanodroplets excited by FUS can induce blood flow occlusion under high pressure, exerting anti-vascular effects and holding tremendous potential for tumor therapy.¹⁰⁶ Additionally, numerous researchers have endeavored to create ultrasound-responsive NPs for diagnostic and therapeutic purposes.

These NPs have the capability to reprogram gene expression,¹⁰⁴ regulate tumor cell metabolism,¹⁰⁷ and modulate the tumor microenvironment (TME).¹⁰⁸ For instance, some researchers developed a tumor microenvironment-responsive nano UCA to increase the proportion of mature dendritic cells and proinflammatory macrophages by reprogramming the metabolism of immature dendritic cells and tumor-associated macrophages (TAMs), which is utilized for chemotherapy and immunotherapy of breast cancer.¹⁰⁸ Throughout this process, PFH within the NPs facilitates monitoring of the treatment corresponding to ultrasound. Qiu Y et al reported on a nano UCA (arsenic trioxide (ATO)/PFH) NPs@Au-cRGD, achieving efficient UI and liver cancer treatment.¹⁰⁹ However, nano UCAs still face several challenges in cancer therapy, including ensuring their stability and biocompatibility *in vivo*, enhancing tumor targeting and specificity, accelerating clinical translation, and so on. With continual advancements and developments in technology, nano UCAs are expected to have an increasingly significant impact on the diagnosis and treatment of cancer.

Photoacoustic Molecular Imaging

PAI stands as a noteworthy clinical imaging technique for the treatment of cancer and other medical conditions, demonstrating considerable advancements over the past decade. Nonetheless, the clinical adoption of PAI-based methodologies continues to face scrutiny due to perceived shortcomings in imaging quality and the clinical information obtained from PA images, which may not always align with findings from alternative imaging modalities. Consequently, efforts to enhance PAI efficacy have pivoted towards the integration of exogenous CAs, typically in the form of nanomaterials, with the aim of achieving superior image quality coupled with reduced side effects, diminished accumulation rates, and enhanced target specificity.¹¹⁰ Materials such as metal NPs, metal sulfide NPs, and semiconductor polymer NPs have found widespread application as photoacoustic CAs.¹¹¹

Metal NPs represent the inaugural materials documented to possess the capability of delivering robust photoacoustic signals.¹¹² Gold NPs are currently regarded as highly efficient optical probes for PAI, owing to their robust extinction coefficients and morphology-dependent optical characteristics. Modulating the size and shape of NPs allows for the adjustment of their localized surface plasmon resonances, thereby facilitating the creation of tailored particles with customized optical properties to serve various purposes.¹¹³ Gold nanorods have traditionally been the preferred choice for PAI due to being the initial anisotropic NPs acquired in the field.¹¹⁴ For example, utilizing functionalized gold nanorods, Alfano et al successfully achieved targeted PAI of bladder cancer based on $\alpha_5\beta_1$.³⁹ Sun IC et al ingeniously exploited the photocatalytic capability of gold nanorods and the photolysis of azides to develop a dual-mode CA named GLANCE. After silica coating and amine functionalization of the gold nanorods, azide compounds were chemically bonded to their surface. GLANCE absorbed NIR laser light and generated nitrogen gas bubbles through the photocatalytic properties of gold nanorods and the photolysis of azide compounds. These bubbles reduced acoustic impedance and accentuated the contrast between the injection site and surrounding tissues, enabling both UI and PAI.⁴⁰ In recent years, there have been other applications of gold NPs for PAI strategies. For instance, gold nanostars have shown promising potential as CAs for photothermal therapy (PTT) and PAI due to their excellent photothermal conversion efficiency. Chen Y et al synthesised gold nanostars without toxic surfactants and coated them with a silica shell to maintain their shape, thus preserving their optical stability. Their outstanding performance was validated through *in vitro* and *in vivo* PAI experiments.⁴¹ Zhang R et al pioneered a novel photoacoustic probe based on a core of nanostars and an outer shell of polymer. Notably, the inclusion of a polymer melanin coating led to a signal enhancement of over fourfold, attributed to its intrinsic photoacoustic capability, thereby improving PAI performance while augmenting biocompatibility. This innovation offers valuable insights for enhancing PAI methodologies.¹¹⁴ However, anisotropic gold NPs such as gold nanorods and gold nanostars exhibit polarization-dependent light absorption, rendering them prone to shape modification into spheres when exposed to pulsed laser irradiation, leading to changes in light absorption and subsequent attenuation of photoacoustic signals, particularly within the NIR window, making anisotropic gold nanostars not ideal for continuous PAI with high imaging contrast. Kim et al demonstrated an effective approach to generate optical responses at NIR wavelengths through plasmon coupling of isotropic gold nanospheres. When two or more gold nanospheres are very close, typically within a few nanometers, their plasmon resonances hybridize, causing the optical absorption peaks to redshift towards longer wavelengths. In the phenomenon of plasmon coupling, the strength of absorption is contingent upon both the quantity and proximity of gold nanospheres. By fabricating a nanoscale superstructure wherein gold nanospheres densely extend

branches in multiple directions, it leads to blackbody-like absorption characteristics at NIR frequencies across various light polarization directions, resulting in robust photoacoustic signals and contrast. The findings demonstrate that such hyper-branched gold nanostructures (HBGNCs) possess notable optical characteristics, including robust NIR absorption, efficient absorption across different polarization angles, and enhanced photostability in comparison to traditional plasmonic CAs like gold nanorods and gold nanospheres. *In vitro* and *in vivo* experiments have confirmed the applicability of HBGNCs as efficient photoacoustic CAs for cancer imaging.¹¹⁵

There are also some other metal NPs used for PAI. Sodium yttrium fluoride doped with ions like ytterbium (Yb^{3+}), erbium (Er^{3+}) and terbium (Tb^{3+}) has been documented for its ability to transform NIR into visible light, facilitating the production of photoacoustic signals that are evaluated in small animal models. Superparamagnetic iron oxide nanoparticles (SPIONs) demonstrated utility in photoacoustic tomography following their encapsulation with a silica coating. Xu Q et al outline the production process of MnO_2 -coated porous Pt@CeO_2 core-shell nanostructures ($\text{Pt@CeO}_2 @\text{MnO}_2$) as an innovative theranostic nano-platform. The porous Pt cores endow the core-shell nanostructures with high photothermal conversion efficiency (80%) in the NIR region, allowing for PTT and PAI of tumors.¹¹⁶ Li L et al reported a high-performance, reversible temperature-responsive PEG-coated tungsten vanadium dioxide ($\text{W-VO}_2 @\text{PEG}$) NP, featuring a robust and switchable NIR-II, enabling greater maximum permissible laser irradiation while reducing light scattering, beneficial for contrast-enhanced PAI in deep-seated diseases.¹¹⁷

Semiconductive polymeric NPs represent a significant portion of organic NPs that exhibit photoacoustic and related properties due to their NIR absorption property. Semiconducting polymers offer unique advantages in photoacoustic applications due to their remarkable photostability and biocompatibility, setting them apart from other NPs. Polymeric NPs containing diketopyrrolopyrrole and its derivatives were utilized for enhanced tumor imaging with more than five times higher than the background signal at 2 h of the NP injection.⁴² Benzothiadiazole moiety doubled the PA signal provided by the NPs.⁴³ Organic dyes are continuously under investigation for its photoacoustic contrast capabilities due to their ability to provide a similar enhancement in PAI as polymeric NPs, while also demonstrating significant biocompatibility.¹¹⁰ Recent studies have found that coupling with phospholipids enhances the effectiveness of porphyrin NPs in PAI. These NPs have also been reported to be a component of photon bubbles, which can serve as CAs for both UI and PAI.¹¹⁸

In conclusion, the combination of PAI technology with NPs enables high-resolution imaging of biological tissues and cells. By using NPs as CAs, the photoacoustic signal can be enhanced, improving imaging sensitivity and resolution.

Multimodal Molecular Imaging

Each imaging technique has its own drawbacks. For example, PET/SPECT are associated with poor spatial resolution and radiation risks, while MRI has relatively low specificity and a long imaging time. In contrast, FI has low spatial resolution and a small penetration depth. Meanwhile, UI has poor resolution and subjective results dependent on the particular operator.⁷² To address these limitations, combining two or more imaging techniques into a new modality—referred to as multimodal molecular imaging—can provide more reliable and accurate information.⁴⁴ This approach leverages the unique strengths and capabilities of different imaging modalities to offer a more complete understanding of biological processes at the molecular level. Currently, most multimodal imaging technologies exhibit dual modalities. The most common combinations, which synergistically enhance detection sensitivity, spatial resolution, biocompatibility, and therapeutic precision, include the fusion of FI with MRI, FI with PAI, and MRI with PAI. We provide a brief overview of NP-based multimodal molecular imaging and its complementary advantages (Figure 3). Multimodal molecular imaging has found extensive application in both preclinical and clinical research, supporting early disease detection, staging, treatment monitoring, surgical guidance, and prognostic evaluation.

Dual-Modality Radionuclide Imaging/MRI

When compared to PET/CT, PET/MRI provides superior soft tissue contrast, lowers radiation exposure, and boosts spatial resolution. The transition from initially employing a mixture of two probes for imaging to the development of PET/MRI probes has been facilitated by the utilization of magnetic NPs, providing a promising avenue. Liolios et al devised a probe, ^{68}Ga -mNP-N1/2, with an IO core, for the assessment of PMSA and gastrin releasing peptide receptor

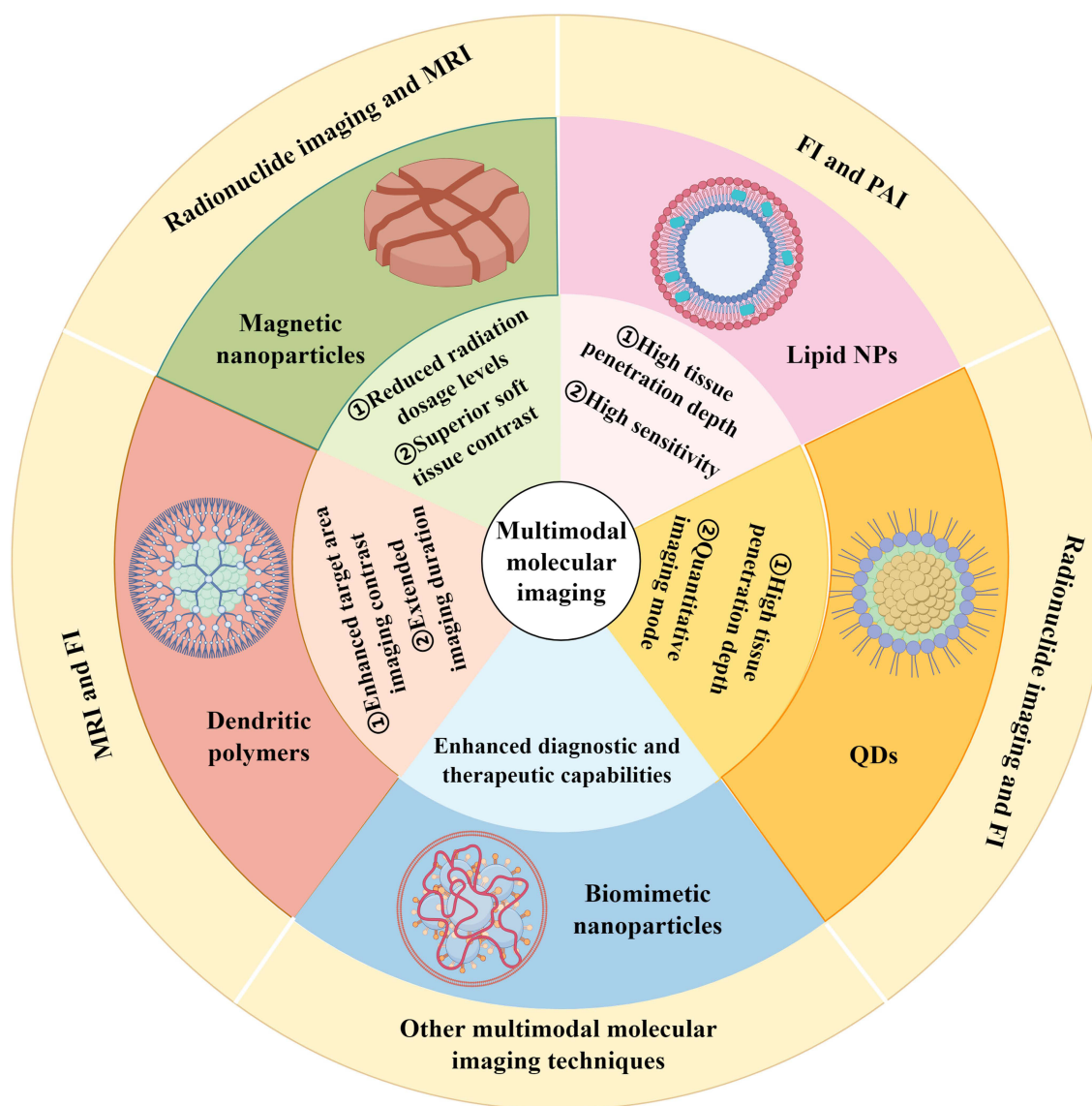


Figure 3 Schematic Diagram of the Design Principles of Activatable Fluorescent Probes (By Figdraw 2.0). The combination of different imaging techniques offers various advantages.

(GRPR) expression. Under the premise of excellent biocompatibility, *in vitro* experiments have yielded specific cell binding.¹¹⁹ Gholipour et al used the amino-thiourea moiety as a chelating agent to prepare probes and nanoprobe binding to $^{68}\text{Ga}^{3+}$ on their surfaces. This probe demonstrates accumulation at the reticuloendothelial system and 4T1 tumor sites (5.4% ID/g).⁸² Several researchers have developed ultrasmall magnetic iron oxide nanoparticles ($^{99\text{m}}\text{Tc}$ -ZW-USIONPs) intrinsically labeled with $^{99\text{m}}\text{Tc}$ through a one-pot synthesis method. Experimental results indicate that these $^{99\text{m}}\text{Tc}$ -ZW-USIONPs exhibit exceptional performance in tumor SPECT and T1-weighted MRI in 4T1 tumor-bearing mice.¹²⁰ Notably, the probe is surface-coated with zwitterionic ions, eliminating the need for chelating agents and preventing protein corona formation. This approach reduces RES uptake, thereby enhancing tumor contrast. The discovery of these nanoprobe indicates that the combination of dual-modal radioactive nuclide imaging and MRI can be used together, complementing each other's strengths to enhance the accuracy and reliability of diagnosis.

Dual-Modality Radionuclide Imaging/FI

The fluorescent signals generated by semiconductor QDs exhibit limited tissue penetration capabilities. Therefore, the development of dual-mode CAs that combine optical imaging with other highly sensitive and quantitative imaging techniques is of significant importance. PET provides complementary advantages and is widely used in early disease detection, malignant tumor staging, and the assessment of treatment responses. Chen K et al were the first to employ amino-functionalized QDs for quantitative examination via NIR FI and PET imaging in tumor-bearing mouse models. The targeted application was achieved through surface modification, which also effectively stabilized the colloidal form of the QDs.¹²¹ Deng H et al developed a multimodal dextran-mimetic quantum dot (Q-Dex) for macrophage imaging. Utilizing NIR emission, this approach enables multimodal imaging through *in vivo* fluorescence, PET, and *ex vivo* as well as *in situ* fluorescence microscopy. Experimental validation demonstrated that, as a macrophage-targeting agent, the Q-Dex probe exhibits excellent targeting at the cellular and tissue levels, with an extended blood half-life.¹²² This advancement paves the way for unprecedented macrophage analysis *in vivo* and diagnostic applications in related diseases such as cancer.

As previously mentioned, using CR generated by radionuclides as the excitation light source for fluorescent probes can achieve deep tissue imaging. The commonly used radioactive metals in dual-modality PET/FI include ⁸⁹Zr, ⁶⁴Cu, and ⁶⁸Ga.¹²³ Shi X et al conjugated folic acid and ICG with DOTA chelation and performed radiolabeling with ⁶⁴Cu to achieve targeted PET and FI of glioblastoma.¹²⁴

Dual-Modality MRI/FI

Integrating FI and MRI within a single nanostructure has been shown to provide powerful imaging capabilities, greatly enhancing the precision of clinical diagnostics. The fundamental design strategy involves combining magnetic NPs with fluorescent and targeting moieties. For instance, dual-mode NPs such as Plectin-SPION-Cy7, utilize SPIONs (Fe₃O₄) conjugated with anti-plectin-1 monoclonal antibodies and Cy7 fluorophores. *In vivo* and *in vitro* experimental data suggest its utility in monitoring pancreatic cancer.¹²⁵ Pan Y et al synthesized fluorescent polymer NPs termed Gd-FPNPs, by a facile one-step etherification copolymerization method. These NPs were conjugated with Gd³⁺ chelates. The results from cell and animal experiments demonstrated excellent biocompatibility and dual-modal FI/MRI capabilities.¹²⁶ In addition, Fu X et al synthesized NPs stabilized by Pluronic F127, which contained ICG and tetra (4-carboxyphenyl) porphyrin-Mn (III) (TCPP(Mn)), serving as a dual-modal probe of FI and MRI. Utilizing F127-ICG/Mn NPs, they successfully distinguished between normal and metastatic sentinel lymph nodes (SLNs) at both microscopic and macroscopic levels via fluorescence imaging and MRI.¹²⁷

Dendritic polymers have been proven to demonstrate superior performance in enhancing imaging contrast in the target area, reducing toxicity, and prolonging imaging duration. A hydrophobic dendritic polymer with multiple Gd³⁺ units developed by researchers, which forms nano micelle reagents at the end, exhibits excellent relaxation properties for MRI. Encapsulating NIR fluorescent dyes within the core of the nanoprobe creates a dual-mode MR/NIR FI reagent, exhibiting efficient MRI performance at lower Gd³⁺ concentrations and allowing for fluorescence intensity more than twice that in NIR imaging.¹²⁸ This holds promising prospects for development.

Dual-Modality FI/PAI

PAI offers high penetration depth and spatial resolution but lower sensitivity, whereas FI provides high sensitivity, temporal and spatial resolution, and SBR but limited penetration capability. The complementary advantages of both modalities make the combination of NIR FI and PAI promising for achieving more precise diagnosis of brain tumors.¹²⁹ Dual-wavelength NIR-II fluorescence and PAI exhibit remarkable spatiotemporal resolution, deep tissue penetration, and high SBR. Guo B et al introduced an innovative approach utilizing conjugated polymer NPs for FI and PAI within the NIR-II window. The NPs possess excellent biocompatibility, superior photostability, and tunable optical properties. By employing FUS to open the blood-brain barrier and NIR-II PAI, these NPs enable the precise localization of microscopic brain tumors smaller than 2 mm in diameter with a high SBR of 7.2. FI allows for the differentiation of blood vessels with a diameter of 23.26 μm at a depth of 600 μm.¹³⁰

The lipid NPs, facile in surface modification and capable of carrying diverse functional payloads while exhibiting excellent biocompatibility, emerge as promising delivery vehicles. However, the complexity introduced by the combination of different functional groups poses challenges for clinical translation. In tackling this challenge, some researchers have pioneered the design of a novel nitrogen-substituted BODIPY-lipid nanoparticle (BODIPYsome).¹³¹ Characterized by a lipid-based nanostructure, this innovative NP showcases unique nanoscale optical properties. Its intact structure demonstrates photoacoustic characteristics, and upon destruction within cancer cells, it restores NIRF properties. The dual PA/FI capability of this NP was observed in *in vivo* animal experiments.

In recent years, research on multi-modal nanoprobes based on AIE has made significant progress. Xu R et al pioneered the development of two AIEgens, namely C-NTBD and O-NTBD, marking the inaugural application of PAI/NIR-II FI in the diagnosis and treatment of neuroendocrine tumors and their SLNs. Notably, under the guidance of NIR-II FI with C-NTBD NPs, even SLNs with a diameter as small as 1 millimeter located distant from the primary tumor site could be detected and accurately excised.¹³²

Other Multimodal Molecular Imaging Techniques

Other multimodal imaging methods are also constantly evolving, such as the combination of MR/PA/FI.^{133,134} Each imaging technique possesses unique characteristics, and the advancement of nanotechnology has propelled the innovation of multimodal molecular imaging technologies. By employing nanostructures, researchers can design multimodal imaging probes, leveraging the complementary attributes of different imaging modalities to enhance diagnostic capabilities. For instance, a single NP may exhibit both magnetic and optical properties, enabling the acquisition of complementary information from MRI and optical imaging modalities. At present, the emphasis in designing and developing multimodal molecular imaging probes lies in the exploration of nanomaterials and the ongoing refinement of probes. For instance, magnetic NPs demonstrate excellent performance in MRI, and their functionality can be enhanced by conjugating targeting moieties and fluorescent tags, thereby conferring FI capabilities. However, existing probes face limitations concerning biocompatibility and stability, such as potential toxicity associated with metallic NPs. In summary, the advancement of multimodal molecular imaging technology provides better support for tumor diagnosis.

Insights from Tumors and Tumor Microenvironment on Nanoparticle-Based Molecular Imaging

TME denotes the microenvironment encompassing tumor cells and their surroundings, which comprise adjacent blood vessels, immune cells, fibroblasts, diverse signaling molecules, and the ECM.¹³⁵ It is shown in Figure 4. The abnormal physiological conditions exhibited by the TME offer a means of distinguishing tumors from normal tissues, serving as a critical basis for the design of molecular imaging probes to enhance tumor targeting. Moreover, NPs might engage with the TME, inducing notable alterations in their characteristics. Concurrently, the TME exerts an impact on the self-assembly or aggregation status of NPs, offering potential utility in devising activatable probes. Improving the microenvironment through NPs can effectively achieve therapeutic goals.

Cancer cells adapt and evolve by altering metabolic pathways, thereby surpassing normal cells and creating a TME that promotes cancer cell survival and metastasis. The robust metabolism of tumor cells and rapid proliferation result in oxidative stress within the cells, leading to a high level of ROS intracellularly. Cells tend to maintain redox homeostasis, hence exhibiting high expression of reduced glutathione (GSH), which is a characteristic feature of tumors. Tumor cells predominantly utilize glucose for glycolysis under aerobic conditions, leading to the accumulation of lactate and ultimately causing acidosis in the extracellular microenvironment. This acidosis, along with oxygen depletion in the surrounding tissues, including immune cells, impairs immune responses and facilitates immune evasion by tumors. The abundance of stimuli leads to abnormalities in growth factors, cytokines, and proteases. The high demand for oxygen also promotes angiogenesis, the formation of new blood vessels.¹³⁶

Hypoxia in TME leads to changes in the expression levels of related factors. High expression of hypoxia-related factors in tumors includes various reductases, cyclooxygenase-2, carbonic anhydrase (CA), GSH, HIF-1 α , providing insights for enzyme-responsive probes.¹³⁷ For example, PET tracer ⁶⁸Ga-NY104 targeting CAIX is currently undergoing

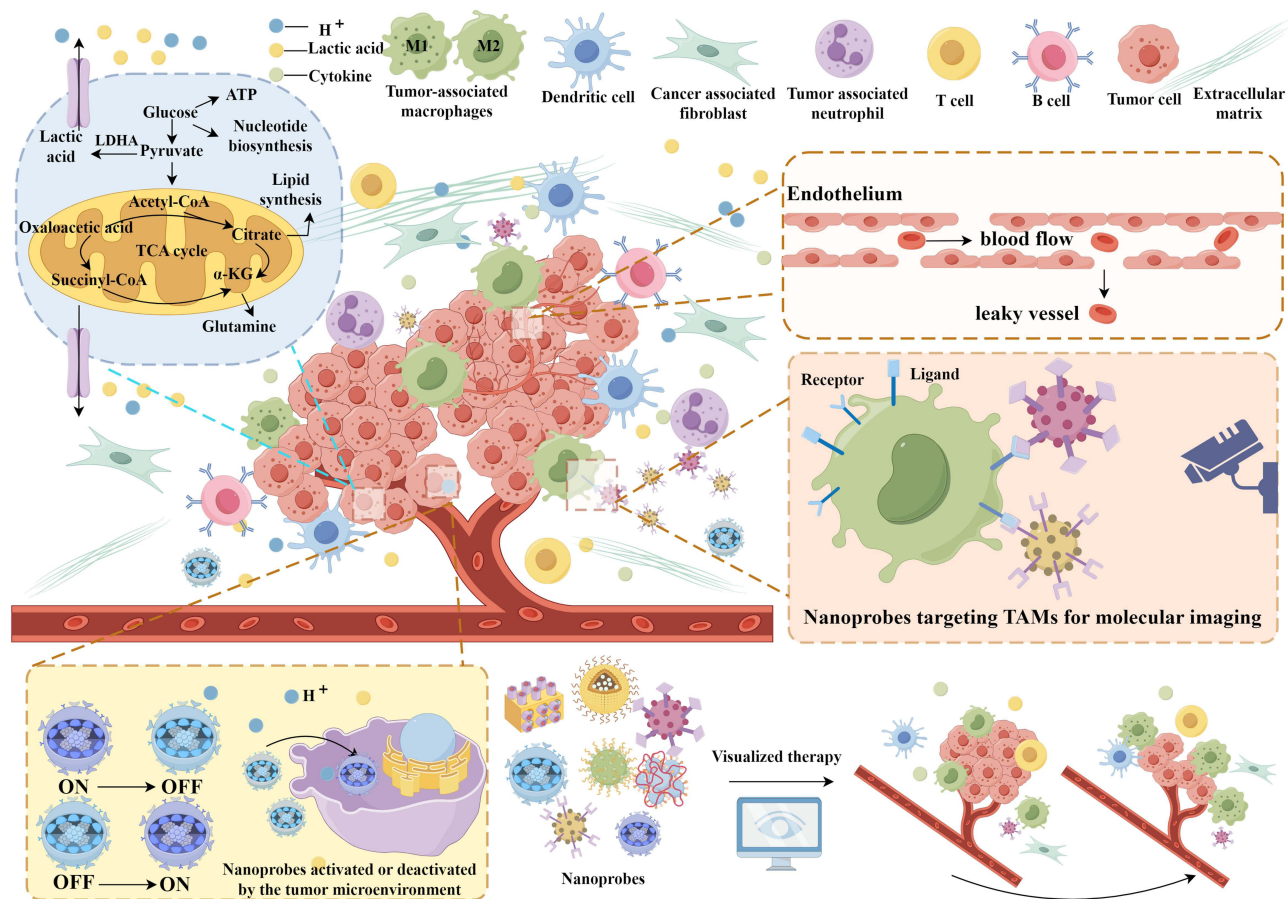


Figure 4 Implications of Tumor Microenvironment Characteristics for the Design of Tumor Imaging Nanoparticles (By Figdraw 2.0). As shown in the center of the figure is the composition of the tumor microenvironment. The upper left corner depicts tumor cells undergoing aerobic glycolysis, producing large amounts of lactic acid, ultimately resulting in an acidic environment. The upper right corner illustrates the formation of incomplete neovasculature within the tumor microenvironment. The middle right section shows the use of targeted cells for molecular imaging, the lower left indicates the design of switchable probes, and the lower right represents the visualization-based treatment using nanoparticle probes.

preclinical and clinical evaluations in tumor, demonstrating its clinical value.¹³⁸ The acidic tumor microenvironment has been extensively employed as an intrinsic stimulus to disrupt pH-labile bonds and trigger material degradation for the release of therapeutic drugs.¹³⁹ Sun R et al obtained SR780@Fe-PAE-COOH by encapsulating pH-responsive polymers into the SR780@Fe. Upon entry into the acidic conditions of tumors, it undergoes degradation, exposing SR780@Fe, which further releases SR780 and Fe³⁺ due to the cleavage of coordination bonds. Through laser irradiation, SR780 promotes cell apoptosis while activating NIR-II FI and PAI. The excessive accumulation of Fe³⁺ facilitates the occurrence of the Fenton reaction, ultimately leading to ferroptosis in cells. Ultimately, this promotes synergistic therapy of tumor visualization through photodynamic and ferroptotic mechanisms.¹⁴⁰ It is worth noting that a study suggests that even slight variations in pH levels may influence the functional properties of NPs on the organism, thus caution needs to be exercised in consideration.¹⁴¹ Tumor angiogenesis is the result of dynamic regulation imbalance, influenced by various growth factors, with VEGFR and $\alpha\beta_3$ being important imaging targets currently under development. On the one side, the immune microenvironment of tumors can be visualized through molecular imaging. For instance, some researchers have designed NPs with NIR absorption and utilized them as cell trackers to observe the directed behavior of macrophages.¹⁴² Conversely, NPs are able to promote immune therapy and monitor treatment. For example, changes in TAMs impact cancer prognosis, with their increase reflecting reduced treatment efficacy. Luo X et al developed a nano-fluorescent probe to monitor the dynamic changes of TAMs induced by low-dose radiotherapy and zoledronic acid, reflecting tumor treatment outcomes.¹⁴³

It is noteworthy that with the advancement of nanobody research, the identification and targeting of TAMs towards deeper regions have become increasingly crucial. Erreni M et al used monovalent (m) or bivalent (biv) forms of anti-Macrophage Mannose Receptor (MMR) nanobodies to evaluate in vivo TAM targeting, conducting a detailed analysis of pharmacokinetics in tumor and healthy tissues, offering crucial insights for future cancer therapy based on nanobody approaches. TAMs with anti-tumor M1-like and pro-tumor M2-like phenotypes coexist in the TME.¹⁴⁴ There has been widespread interest in reprogramming TAMs to alter the tumor immune-suppressive microenvironment. Chong L et al engineered biomimetic NPs to promote the transition of M2-like TAMs to M1-like TAMs. Under acidic conditions in the tumor, the probe can degrade to produce Mn^{2+} for MRI, enabling tumor tracking.¹⁴⁵

Table 2 Clinical Trials of Nanoparticles in Tumor Molecular Imaging

Type	Agent and modality	Investigated motivation/indication	Status	Clinical Trials. gov identifiers
Sulfur Colloid	^{99m} Tc, SPECT	Investigate whether alkalinization of ^{99m} Tc-sulfur colloid capsules can reduce the level of pain perception during non-breast sentinel lymph node imaging procedures	Completed Has results	NCT01660412
Sulfur Colloid	^{99m} Tc, SPECT	Detecting the spread of oral or throat cancer to the neck lymph nodes in patients.	Completed	NCT00012168
Gold	Nanoshell, photothermal	AuroLase (TM) treats patients with refractory and/or recurrent head and neck tumors.	Completed Has results	NCT00848042
Gold Nanoparticles	CD24, qPCR	Early detection of cancer stem cells in salivary gland tumors using CD24 coupled gold nanoparticles	Completed	NCT04907422
Silica Nanomolecular Particle	¹²⁴ I, PET	Study on using ¹²⁴ I-labeled cRGDY mesoporous silica nanoparticles as a tracer for PET imaging in patients with melanoma and malignant brain tumors.	Active, not recruiting	NCT01266096
Iron Oxide	Ferumoxytol, MRI	Describe the quantitative imaging changes of brain tumor blood vessels after anti angiogenic therapy and steroid therapy	Terminated	NCT00769093
Superparamagnetic Iron Oxide (SPIO)	Feraheme, MRI	Detecting lymph node metastasis of pancreatic cancer using superparamagnetic iron oxide magnetic resonance imaging	Completed Has results	NCT00920023
Superparamagnetic Particles of Iron Oxide	Ferumoxide, MRI	In vivo tracking of magnetic labeled implanted stem cells using MRI scanning	Completed	NCT01169935
Ultra-small Superparamagnetic Iron Oxide	Ferumoxytol, MRI	Imaging of myocarditis after acute myocardial infarction	Completed	NCT01995799
Ultra-small Superparamagnetic Iron Oxide	Ferumoxtran-10, MRI	Evaluate the pathological impact of USPIO-MRI on patients with pancreatic cancer or periampullary cancer.	Terminated	NCT04311047
Ultra-small Superparamagnetic Iron Oxide	Ferumoxtran-10, MRI ⁶⁸ Ga PSMA PET-CT	Verify the accuracy of ⁶⁸ Ga PSMA PET-CT and USPIO-MRI prostate cancer lymph node imaging	Unknown	NCT03223064
Polysiloxane Gd-Chelates based nanoparticles	AGuIX, SBRT	To determine the safety and effectiveness of Ga-based nanoparticles AGuIX (Activation and Guidance of Irradiation X) in combination with magnetic resonance guided stereotactic radiotherapy (SBRT) in the treatment of pancreatic cancer and lung tumors.	Ongoing	NCT04789486

New Applications in Tumor Molecular Imaging

Currently, various NP-based drugs have entered clinical research on tumor molecular imaging. We have summarized recent developments in the clinical application of NPs in molecular imaging in [Table 2](#), demonstrating significant potential applications. Nano drug carriers exhibit the capacity for precision drug delivery within the organism, enhancing therapeutic efficacy. Additionally, treatment response can be monitored through imaging techniques. This integrated approach to treatment and diagnosis is commonly referred to as “theranostics”. Here, we provide a concise summary of the integrated tumor diagnosis and therapy platform based on the NP technology, along with its current development status.

Image-guided Surgery

The initiation of a new era in image-guided surgery was marked by the pioneering NIR-II fluorescence-assisted human liver tumor operation. This advancement underscores the transformative impact of molecular imaging in surgical precision and patient outcomes.¹⁴⁶ During tumor resection surgeries, surgeons commonly rely on visual observation and tactile sensation to locate the position of tumor and determine the boundary of resection. However, discerning tumor margins from surrounding normal tissue at a macroscopic level is often challenging. Intraoperative margin assessment is typically conducted using frozen section analysis and imprint cytology. While these methods hold promise in reducing positive margin rates, they are laborious, time-consuming, and inherently limited in sensitivity because of limitations in sampling rates. Intraoperative imaging offers advantages in overcoming these challenges by enabling identification of small malignant tumors that may not be detected preoperatively using conventional imaging techniques, and by facilitating real-time assessment of residual lesions and surgical margins within the operating room.

In FI, selecting the optimal fluorescent probe is crucial for achieving higher TNR (tumor-to-normal tissue ratio). Xu H et al utilized rigid polystyrene NPs as carriers to load AIEgens, thereby constructing highly luminescent nano-probes. Experimental results demonstrate that NIR-II@ polystyrene nano-probes exhibit exceptional accuracy in defining the boundaries of small peritoneal tumor nodules, attributed to reduced interaction between light and tissue and improved spatial resolution of NIR-II light, resulting in high TNR.¹⁴⁷ This technology holds vast potential for accurately resecting tiny metastatic lesions in fluorescence-guided surgical procedures.

In addition to fluorescence-guided tumor surgery, PAI holds advantages for the resection of deep-seated tumors due to its high tissue penetration depth. For instance, Yu Q et al utilized PAI employing endogenous melanin as a contrast to target and eliminate B16 melanoma liver metastases. Hepatic melanoma as small as 400 μm in diameter in the liver could be detected up to a depth of 7 mm, and precise resection guided by PAI demonstrated its advantages, including high resolution, sensitivity, deep tissue penetration, and early detection of liver micrometastases.¹⁴⁸ Similarly, Liu JJ et al utilized a PAI method employing melanin NPs conjugated with cyclic Arg-Gly-Asp (cRGD) for improved detection and accurate resection of breast cancer.¹⁴⁹

Image-guided Photodynamic Therapy

PDT is a modern non-invasive therapy that requires the concentration of a photosensitizer in tumor tissue, followed by irradiation of the tumor site with light of a specific wavelength.¹⁵⁰ This process generates ROS with cytotoxic effects, thereby achieving tumor cell destruction. However, the application of PDT is limited by adverse factors in the TME, such as the elevated levels of GSH, which are approximately four times higher than those in normal tissues. Numerous research efforts have aimed to diminish the level of GSH in the TME to augment the effectiveness of PDT. Nanozymes, which possess both nano-material and natural enzyme characteristics, provide a promising approach to improve PDT efficacy. Feng S et al first discovered that mesoporous carbon has a glutathione oxidase-like activity that depletes GSH, and they found that the depletion of GSH enhanced the efficacy of PDT by loading Ce6 onto mesoporous carbon.¹⁵¹ Subsequently, they prepared Cu^{2+} doped carbon NPs (CHC) loaded with photosensitisers for the combined treatment of metastatic tumors. They coated the surface of CHC with hyaluronic acid, which was broken down when it reached the tumor site and encountered hyaluronidase overexpression, allowing the catalytic activity of CHC to be selectively exerted. When exposed to NIR, the accumulation of CHC at the tumor location results in the production of heat in

that specific area, leading to the targeted induction of apoptosis in tumor cells, while enhancing the photodynamic effect and enzyme-like activity. FI reflected the protective effect of NPs on photosensitisers.

Hypoxia also limits the efficacy of PDT, and improving hypoxia has become a focus of research. Ruthenium (Rh)-based nanostructures have been explored as potential biocompatible materials for NIR absorption in tumor PTT. Moreover, rhodium exhibits inherent catalase-like activity, capable of decomposing H_2O_2 into O_2 . Wang J et al synthesized porous Au@Rh core-shell structures as a fundamental platform, with ICG loaded into the pores and coated with cancer CMs to form Au@Rh-ICG-CM nanocomposites. When exposed to 808 nm laser irradiation, Au@Rh-ICG-CM facilitates the catalytic decomposition of H_2O_2 , improving hypoxia and enhancing PDT therapy. Additionally, FI/PAI allows for monitoring the distribution of Au@Rh-ICG-CM within tissues and aids in directing the therapeutic interventions.¹⁵²

Image-guided Chemodynamic Therapy

Chemodynamic therapy (CDT) involves the use of Fenton or Fenton-like reaction to produce extremely cytotoxic $\bullet\text{OH}$ from H_2O_2 with the aim of eradicating cancer cells. This approach demonstrates considerable therapeutic potential in the treatment of tumors.¹⁵³ To date, the nanocatalysts that have been subject to the most comprehensive research are still those derived from Fe, including Fe_3O_4 , FeS_2 , and ferrocene-based NPs. This is primarily due to the notable catalytic efficacy exhibited by $\text{Fe}^{3+}/\text{Fe}^{2+}$.^{154,155} Fe^{2+} is prone to oxidation, leading to systemic adverse effects. Hence, the development of a manageable Fe^{2+} delivery system poses a difficulty in preserving its valence state, mitigate toxicity, and improving therapeutic effectiveness. He T et al reported a NIR light-triggered Fe^{2+} delivery agent (LET-6). Under the guidance of FI and PAI, the thermal expansion induced by 808 nm laser irradiation triggers the transformation of LET-6, exposing Fe^{2+} from its hydrophobic layer. This subsequently catalyzes the degradation of endogenous H_2O_2 in TME, generating $\bullet\text{OH}$ and enhancing CDT efficacy.¹⁵⁶ This lays the groundwork for forthcoming collaborative approaches in cancer therapy involving metal ions. Besides, other metal-based nanocatalysts, such as Mn^- , Cu^- , Co^- , and Ag-based nanomaterials, have been synthesized for applications in Fenton-like chemical reactions. Yang L et al engineered multifunctional MOF NPs with dual capabilities. These MOFs utilize redox-active copper-based units to catalyze the conversion of H_2O_2 to $\bullet\text{OH}$, and also emit characteristic NIR luminescence through Yb_4 clusters embedded in the scaffold.¹⁵⁷ Research has confirmed the dual functionality of MOF NPs. In another work, Zhang Z et al developed a biodegradable nanosystem ($\text{Ag}_2\text{S-GOx@BHS NYs}$) with the aim of facilitating tumor therapy through the induction of ROS.¹⁵⁸

CDT is also influenced by TME, and single therapeutic modalities have inherent limitations. Integrating different treatment methods into a single nanocarrier platform can significantly enhance cancer therapy effectiveness. For instance, An G et al established a MOF using surface-modified copper NPs to eliminate tumors through multiple cascading synergistic therapeutic effects. Nanotherapy with cerium exhibits outstanding oxidative and reductive capabilities, facilitating reversible conversion between Ce^{4+} and Ce^{3+} to transform H_2O_2 into $\bullet\text{OH}$. Similar to Cu^{2+} , Ce^{4+} also accelerates GSH consumption through redox reactions, thereby diminishing its efficacy in scavenging $\bullet\text{OH}$. Additionally, external energy fields like heat and ultrasound adjunctively enhance the Fenton/Fenton-like reaction for boosting ROS.¹⁵⁹

Immunogenic cell death (ICD) is recognized as a programmed form of cellular demise that provides a significant theoretical framework for tumor immunotherapy. Cheng M et al devised a straightforward, one-step strategy for synthesizing multifunctional copper-cerium oxide NPs (mCu&Ce) featuring mesoporous nanostructures. After encapsulating ICG and surface grafting with RGD (Arg-Gly-Asp) peptide, this nanoplatform accurately targets osteosarcoma and triggers the release of ICG, copper, and cerium ions within the TME (pH = 6.5). Subsequently, the NPs efficiently generate hyperthermia and sequentially enhance $\bullet\text{OH}$ production under NIR laser irradiation. This approach enables PTT/CDT both in vitro and in vivo. Furthermore, heat and augmented ROS are critical factors in improving the effectiveness of tumor immunotherapy through ICD induction, fostering potent T cell development and triggering a robust immune response against osteosarcoma.¹⁶⁰ Moreover, the Cu&Ce-based nanoplatform enables accurate early detection of osteosarcoma through NIR-II FI and MRI.

The integration of therapeutic and diagnostic modalities, from the initial conceptualization of theranostics to the establishment of multifunctional nanoplatforms, offers promising prospects for the precise targeting of tumors. An

increasing number of researchers are also continuously developing novel approaches for cancer treatment, such as PTT, ferroptosis therapy, sonodynamic therapy, immunotherapy, and gene therapy, all of which hold promising prospects for further development.^{161–164}

Summary and Outlook

Molecular imaging provides visual and quantitative support for in-depth tumor research, enabling early diagnosis and the potential for precision medicine. The advancements in molecular imaging technologies not only involve the development of new techniques but also the research and development of probes/contrast agents. The characteristics of probes/contrast agents vary depending on the technology being employed. In recent years, with the maturation of multimodal fusion imaging technologies, multimodal imaging has emerged as a significant trend, particularly in the development of theranostic probes, which better meet clinical demands and facilitate precision medicine. However, molecular imaging still faces numerous clinical challenges, such as the difficulty in standardizing probe preparation, which raises concerns about biosafety and increases the pressure of clinical translation. Additionally, the reliability of molecular imaging results still requires validation through other diagnostic methods, such as pathology.

To date, nanotechnology has been extensively employed in molecular imaging, with notable advancements in the diagnosis and treatment of tumors. Nanotechnology has many potential advantages in molecular imaging applications, such as high resolution, targeting, and versatility. With the development and integration of nanotechnology, biomedicine, chemical materials science and artificial intelligence, multifunctional nanodrugs with stronger stability, higher safety and more precise targeting have emerged. However, nanotechnology has some limitations. For example, nanotechnology is still in the development stage in the field of molecular imaging, and some nanoimaging technologies have not yet reached the mature level of clinical applications. Most of the current understanding of the distribution and metabolic mechanisms of NPs in vivo comes from animal experimental data, and there are very few studies conducted to transplant these behaviors into humans. Over the past few years, researchers have devoted significant resources to the application of nanomaterials in molecular imaging, with the goal of developing more effective treatments for human diseases.

In the future, we should pay attention to the design and construction of new, efficient, and safe multi-functional integrated nanomaterials, and study the distribution, stability, biocompatibility and biotoxicity of nanomaterials in the living body to develop suitable nanomolecular imaging probes and enhance imaging quality, thereby ensuring effective diagnosis and treatment of tumors. In general, the future development of nanotechnology in molecular imaging applications is expected to completely transform the fields of medical diagnosis, treatment, and disease monitoring.

Abbreviations

AIE, aggregation-induced emission; AIEgen, aggregation-induced emission luminogen; ALP, alkaline phosphatase; BLI, bioluminescence imaging; CAFs, cancer-associated fibroblasts; CA, carbonic anhydrase; CAs, contrast agents; Ce6, Chlorin e6; CEST, Chemical exchange saturation transfer; CEST, contrast-enhanced ultrasound; CMs, cell membranes; CR, cherenkov radiation; CRET, cherenkov radiation energy transfer; DOX, doxorubicin; ECM, extracellular matrix; ED-B FN, extra domain-B fibronectin; FDA, Food and Drug Administration; FI, fluorescence imaging; FRET, Förster resonance energy transfer; 5-FU, 5-fluorouracil; FUS, focused ultrasound; NPs, nanoparticles; MRI, magnetic resonance imaging; UI, ultrasound imaging; PAI, photoacoustic imaging; QDs, quantum dots; SPECT, Single Photon Emission Computed Tomography; PET, Positron Emission Tomography; IO, Iron oxide; PEI, polyethylenimine; PEG, polyethylene glycol; PEG-PLA, polyethylene glycol-poly(lactic acid); PDT, photodynamic therapy; NIRF, near-infrared fluorescence; NIR, near-infrared; ICG, indocyanine green; SBR, signal-to-background ratio; SNR, signal-to-noise ratio; PeT, photo-induced electron transfer; RTP, room-temperature phosphorescence; GBCAs, gadolinium-based contrast agents; Gd-CDs, Gd-doped carbon dots; Gd-DTPA, gadolinium diethylenetriamine pentaacetate; PDA, polydopamine; MOFs, magnetic metal-organic frameworks; UHF, ultra-high field; UCAs, ultrasound contrast agents; NBs, nanobubbles; GVs, gas vesicles; PFC, perfluorocarbon; PFH, perfluorohexane; GLUL, glutamine synthetase; TAMs, tumor-associated macrophages; PTT, photothermal therapy; HBGNCs, hyper-branched gold nanostructures; SPIONs, Superparamagnetic iron oxide nanoparticles; GRPR, gastrin releasing peptide receptor; Q-Dex, dextran-mimetic quantum dots; SLNs, sentinel lymph nodes; TME, tumor microenvironment; ROS, reactive oxygen species; GSH, glutathione; cRGD, cyclic Arg-Gly-

Asp; RGD, Arg-Gly-Asp; MMR, macrophage mannose receptor; TNR, tumor-to-normal tissue ratio; CDT, chemodynamic therapy; ICD, immunogenic cell death; Eu, Europium; Gd, gadolinium; Ho, Holmium; Yb, ytterbium; Er, erbium; terbium; Tb, Lu, Lutetium; Re, Rhenium; In, Indium; Zr, Zirconium.

Data Sharing Statement

All data generated or analyzed during this study are included in this published article.

Acknowledgments

This work was supported by the National Natural Science of Foundation of China (82102096) and Science and Technology Development Plan of Jilin (20240101275JC and YDZJ202401200ZYTS).

Disclosure

The authors report no conflicts of interest in this work.

References

1. Sung H, Ferlay J, Siegel RL, et al. Global cancer statistics 2020: globocan estimates of incidence and mortality worldwide for 36 cancers in 185 countries. *CA Cancer J Clin.* 2021;71(3):209–249. doi:10.3322/caac.21660
2. Rowe SP, Pomper MG. Molecular imaging in oncology: current impact and future directions. *CA Cancer J Clin.* 2022;72(4):333–352. doi:10.3322/caac.21713
3. Dilsizian V, Chandrashekar Y. Molecular Imaging: new Promises. *JACC Cardiovasc Imaging.* 2022;15(11):2019–2021. doi:10.2147/IJN.S215137
4. Woźniak M, Płoska A, Siekierzycka A, Dobrucki LW, Kalinowski L, Dobrucki IT. Molecular imaging and nanotechnology-emerging tools in diagnostics and therapy. *Int J Mol Sci.* 2022;23(5). doi:10.3390/ijms23052658
5. Joudeh N, Linke D. Nanoparticle classification, physicochemical properties, characterization, and applications: a comprehensive review for biologists. *J Nanobiotechnol.* 2022;20(1):262. doi:10.1186/s12951-022-01477-8
6. Ghosh T, Nandi S, Bhattacharyya SK, et al. Nitrogen and sulphur doped carbon dot: an excellent biocompatible candidate for in-vitro cancer cell imaging and beyond. *Environ Res.* 2023;217:114922. doi:10.1016/j.envres.2022.114922
7. Ghosh T, Sahoo R, Ghosh SK, Banerji P, Das NC. Simplistic hydrothermal synthesis approach for fabricating photoluminescent carbon dots and its potential application as an efficient sensor probe for toxic lead (II) ion detection. *Front Chem Sci Eng.* 2023;17(5):536–547. doi:10.1007/s11705-022-2239-y
8. Jakerst JV, Gambhir SS. Molecular imaging with theranostic nanoparticles. *Acc Chem Res.* 2011;44(10):1050–1060. doi:10.1021/ar200106e
9. Liu S-Y, S-N L, Lee W-C, Hsu W-C, Lee T-W, Chang C-H. Evaluation of nanotargeted 111In-cyclic RGDfK-liposome in a human melanoma xenotransplantation model. *Int J Mol Sci.* 2021;22(3):1099. doi:10.3390/ijms22031099
10. Goos J, Cho A, Carter LM, et al. Delivery of polymeric nanostars for molecular imaging and endoradiotherapy through the enhanced permeability and retention (EPR) effect. *Theranostics.* 2020;10(2):567–584. doi:10.7150/thno.36777
11. Jang HM, Jung MH, Lee JS, et al. Chelator-free copper-64-incorporated iron oxide nanoparticles for pet/mr imaging: improved radiocopper stability and cell viability. *Nanomaterials.* 2022;12(16):2791. doi:10.3390/nano12162791
12. Xiao L, Li Y, Geng R, et al. Polymer composite microspheres loading (177)Lu radionuclide for interventional radioembolization therapy and real-time SPECT imaging of hepatic cancer. *Biomater Res.* 2023;27(1):110. doi:10.1186/s40824-023-00455-x
13. Choi PS, Lee JY, Chae JH, et al. Theranostics through utilizing cherenkov radiation of radioisotope Zr-89 with a nanocomposite combination of TiO(2) and MnO(2). *ACS Appl Mater Interf.* 2023;15(3):3689–3698. doi:10.1021/acsami.2c09195
14. Mendes Miranda SE, Alcântara Lemos J, Fernandes RS, et al. Enhanced antitumor efficacy of lapachol-loaded nanoemulsion in breast cancer tumor model. *Biomed Pharmacother.* 2021;133:110936. doi:10.1016/j.biopha.2020.110936
15. Katifelis H, Mukha I, Bouziotis P, et al. Ag/Au bimetallic nanoparticles inhibit tumor growth and prevent metastasis in a mouse model. *Int J Nanomed.* 2020;15:6019–6032. doi:10.2147/ijn.S251760
16. Kato H, Huang X, Kadonaga Y, et al. Intratumoral administration of astatine-211-labeled gold nanoparticle for alpha therapy. *J Nanobiotechnol.* 2021;19(1):223. doi:10.1186/s12951-021-00963-9
17. Wang Z, Ye M, Ma D, Shen J, Fang F. Engineering of (177)Lu-labeled gold encapsulated into dendrimeric nanomaterials for the treatment of lung cancer. *J Biomater Sci Polym Ed.* 2022;33(2):197–211. doi:10.1080/09205063.2021.1982446
18. Sun N, Zhao L, Zhu J, et al. (131)I-labeled polyethylenimine-entrapped gold nanoparticles for targeted tumor SPECT/CT imaging and radionuclide therapy. *Int J Nanomed.* 2019;14:4367–4381. doi:10.2147/ijn.S203259
19. Yan R, Hu Y, Liu F, et al. Activatable NIR fluorescence/MRI bimodal probes for in vivo imaging by enzyme-mediated fluorogenic reaction and self-assembly. *J Am Chem Soc.* 2019;141(26):10331–10341. doi:10.1021/jacs.9b03649
20. Liu J, Li M, Dang Y, Lou H, Xu Z, Zhang W. NIR-I fluorescence imaging tumorous methylglyoxal by an activatable nanoprobe based on peptide nanotubes by FRET process. *Biosens Bioelectron.* 2022;204:114068. doi:10.1016/j.bios.2022.114068
21. Xu L, Gao H, Deng Y, et al. β -Galactosidase-activated near-infrared AIEgen for ovarian cancer imaging in vivo. *Biosens Bioelectron.* 2024;255:116207. doi:10.1016/j.bios.2024.116207
22. Qu Q, Zhang Z, Guo X, et al. Novel multifunctional NIR-II aggregation-induced emission nanoparticles-assisted intraoperative identification and elimination of residual tumor. *J Nanobiotechnol.* 2022;20(1):143. doi:10.1186/s12951-022-01325-9

23. Chang K, Xiao L, Fan Y, et al. Lighting up metastasis process before formation of secondary tumor by phosphorescence imaging. *Sci Adv.* 2023;9(20):eadf6757. doi:10.1126/sciadv.adf6757
24. Shi Y, Xia Y, Zhou M, et al. Facile synthesis of Gd/Ru-doped fluorescent carbon dots for fluorescent/MR bimodal imaging and tumor therapy. *J Nanobiotechnol.* 2024;22(1):88. doi:10.1186/s12951-024-02360-4
25. Valimukhametova AR, Zub OS, Lee BH, et al. Dual-mode fluorescence/ultrasound imaging with biocompatible metal-doped graphene quantum dots. *ACS Biomater Sci Eng.* 2022;8(11):4965–4975. doi:10.1021/acsbiomaterials.2c00794
26. Zhu J, Chu H, Shen J, Wang C, Wei Y. Carbon quantum dots with pH-responsive Orange-/red-light emission for fluorescence imaging of intracellular pH. *Mikrochim Acta.* 2023;190(1):21. doi:10.1007/s00604-022-05605-x
27. Du J, Zhou S, Ma Y, et al. Folic acid functionalized gadolinium-doped carbon dots as fluorescence/magnetic resonance imaging contrast agent for targeted imaging of liver cancer. *Colloids Surf B.* 2024;234:113721. doi:10.1016/j.colsurfb.2023.113721
28. Liu S, Jiang Y, Liu P, et al. Single-atom gadolinium nano-contrast agents with high stability for tumor T1 magnetic resonance imaging. *ACS nano.* 2023;17(9):8053–8063. doi:10.1021/acsnano.2c09664
29. Ma G, Zhang X, Zhao K, et al. Polydopamine nanostructure-enhanced water interaction with pH-responsive manganese sulfide nanoclusters for tumor magnetic resonance contrast enhancement and synergistic ferroptosis–photothermal therapy. *ACS nano.* 2024;18.
30. Pan X, Lu Y, Fan S, et al. Gold nanocage-based multifunctional nanosensitizers for programmed photothermal/radiation/chemical coordinated therapy guided by FL/MR/PA multimodal imaging. *Int J Nanomed.* 2023. 7237–7255. doi:10.2147/IJN.S436931
31. Fan Y, Chen D, Chen L, et al. Fluorinated iron metal–organic frameworks for activatable 19f magnetic resonance imaging and synergistic therapy of tumors. *Nano Lett.* 2023;23(24):11989–11998. doi:10.1021/acsnanolett.3c04402
32. Liang Z, Xiao L, Wang Q, et al. Ligand-mediated magnetism-conversion nanoprobes for activatable ultra-high field magnetic resonance imaging. *Angew Chem.* 2024;136(10):e202318948. doi:10.1002/ange.202318948
33. Zhang R, Liu M, Liu S, et al. Holmium (III)-doped multifunctional nanotheranostic agent for ultra-high-field magnetic resonance imaging-guided chemo-photothermal tumor therapy. *Acta Biomater.* 2023;172:454–465. doi:10.1016/j.actbio.2023.10.017
34. Wang Y, De Leon AC, Perera R, et al. Molecular imaging of orthotopic prostate cancer with nanobubble ultrasound contrast agents targeted to PSMA. *Sci Rep.* 2021;11(1):4726. doi:10.1038/s41598-021-84072-5
35. Mi X, Guo X, Du H, et al. Combined legumain- and integrin-targeted nanobubbles for molecular ultrasound imaging of breast cancer. *Nanomedicine.* 2022;42:102533. doi:10.1016/j.nano.2022.102533
36. Wei M, Lai M, Zhang J, Pei X, Yan F. Biosynthetic gas vesicles from halobacteria NRC-1: a potential ultrasound contrast agent for tumor imaging. *Pharmaceutics.* 2022;14(6):1198. doi:10.3390/pharmaceutics14061198
37. Zhang G, Liao C, Hu JR, et al. Nanodroplet-based super-resolution ultrasound localization microscopy. *ACS Sens.* 2023;8(9):3294–3306. doi:10.1021/acssensors.3c00418
38. Maghsoudinia F, Tavakoli MB, Samani RK, et al. Folic acid-functionalized gadolinium-loaded phase transition nanodroplets for dual-modal ultrasound/magnetic resonance imaging of hepatocellular carcinoma. *Talanta.* 2021;228:122245. doi:10.1016/j.talanta.2021.122245
39. Alfano M, Alchera E, Sacchi A, et al. A simple and robust nanosystem for photoacoustic imaging of bladder cancer based on $\alpha 5\beta 1$ -targeted gold nanorods. *J Nanobiotechnol.* 2023;21(1):301. doi:10.1186/s12951-023-02028-5
40. Sun I-C, Dumani DS, Emelianov SY. Applications of the photocatalytic and photoacoustic properties of gold nanorods in contrast-enhanced ultrasound and photoacoustic imaging. *ACS nano.* 2024;18(4):3575–3582. doi:10.1021/acsnano.3c11223
41. Chen Y, Xu C, Cheng Y, Cheng Q. Photostability enhancement of silica-coated gold nanostars for photoacoustic imaging guided photothermal therapy. *Photoacoustics.* 2021;23:100284. doi:10.1016/j.pacs.2021.100284
42. Jiang S, Lin J, Huang P. Nanomaterials for NIR-II Photoacoustic Imaging. *Adv Healthcare Mater.* 2023;12(16):2202208. doi:10.1002/adhm.202202208
43. Zhen X, Pu K, Jiang X. Photoacoustic imaging and photothermal therapy of semiconducting polymer nanoparticles: signal amplification and second near-infrared construction. *Small.* 2021;17(6):2004723. doi:10.1002/smll.202004723
44. Bai JW, Qiu SQ, Zhang GJ. Molecular and functional imaging in cancer-targeted therapy: current applications and future directions. *Signal Transduct Target Ther.* 2023;8(1):89. doi:10.1038/s41392-023-01366-y
45. Kiraga L, Kucharzewska P, Paisey S, et al. Nuclear imaging for immune cell tracking in vivo—Comparison of various cell labeling methods and their application. *Coord Chem Rev.* 2021;445:214008. doi:10.1016/j.ccr.2021.214008
46. Rong J, Haider A, Jeppesen TE, Josephson L, Liang SH. Radiochemistry for positron emission tomography. *Nat Commun.* 2023;14(1):3257. doi:10.1038/s41467-023-36377-4
47. Karageorgou MA, Bouziotis P, Stiliaris E, Stamopoulos D. Radiolabeled iron oxide nanoparticles as dual modality contrast agents in SPECT/MRI and PET/MRI. *Nanomaterials.* 2023;13(3):503. doi:10.3390/nano13030503
48. Rainone P, De Palma A, Sudati F, et al. (99m)Tc-Radiolabeled Silica Nanocarriers for Targeted Detection and Treatment of HER2-Positive Breast Cancer. *Int J Nanomed.* 2021;16:1943–1960. doi:10.2147/ijn.S276033
49. Wu P, Zhu H, Zhuang Y, Sun X, Gu N. Combined therapeutic effects of (131)I-labeled and 5fu-loaded multifunctional nanoparticles in colorectal cancer. *Int J Nanomed.* 2020;15:2777–2787. doi:10.2147/ijn.S215137
50. Roy I, Krishnan S, Kabashin AV, Zavestovskaya IN, Prasad PN. Transforming nuclear medicine with nanoradiopharmaceuticals. *ACS nano.* 2022;16(4):5036–5061. doi:10.1021/acsnano.1c10550
51. Gong Z, Chen J, Chen R, et al. Interfacial Cherenkov radiation from ultralow-energy electrons. *Proc Natl Acad Sci U S A.* 2023;120(38):e2306601120. doi:10.1073/pnas.2306601120
52. Guo R, Jiang D, Gai Y, et al. Chlorin e6-loaded goat milk-derived extracellular vesicles for Cerenkov luminescence-induced photodynamic therapy. *Eur J Nucl Med Mol Imaging.* 2023;50(2):508–524. doi:10.1007/s00259-022-05978-4
53. Lengacher R, Martin KE, Śmiłowicz D, et al. Targeted, molecular europium(III) probes enable luminescence-guided surgery and 1 photon post-surgical luminescence microscopy of solid tumors. *J Am Chem Soc.* 2023;145(44):24358–24366. doi:10.1021/jacs.3c09444
54. Hilderbrand SA, Weissleder R. Near-infrared fluorescence: application to in vivo molecular imaging. *Curr Opin Chem Biol.* 2010;14(1):71–79. doi:10.1016/j.cbpa.2009.09.029
55. Gioux S, Choi HS, Frangioni JV. Image-guided surgery using invisible near-infrared light: fundamentals of clinical translation. *Molecular Imaging.* 2010;9(5):7290.2010.00034. doi:10.2310/7290.2010.00034

56. Orosco RK, Tsien RY, Nguyen QT. Fluorescence imaging in surgery. *IEEE Revi Biomedical Engine.* 2013;6:178–187. doi:10.1109/RBME.2013.2240294
57. Van Dam GM, Themelis G, Crane LM, et al. Intraoperative tumor-specific fluorescence imaging in ovarian cancer by folate receptor- α targeting: first in-human results. *Nature Med.* 2011;17(10):1315–1319. doi:10.1038/nm.2472
58. Mondal SB, Gao S, Zhu N, Liang R, Grucev V, Achilefu S. Real-time fluorescence image-guided oncologic surgery. *Adv Cancer Res.* 2014;124:171–211.
59. Ji Y, Jones C, Baek Y, Park GK, Kashiwagi S, Choi HS. Near-infrared fluorescence imaging in immunotherapy. *Adv. Drug Delivery Rev.* 2020;167:121–134. doi:10.1016/j.addr.2020.06.012
60. Vahrmeijer AL, Hutteman M, van der Vorst JR, van de Velde CJ, Frangioni JV. Image-guided cancer surgery using near-infrared fluorescence. *Nat Rev Clin Oncol.* 2013;10(9):507–518. doi:10.1038/nrclinonc.2013.123
61. Dai L, Zhang Q, Ma Q, Lin W. Emerging near infrared fluorophore: dicyanoisophorone-based small-molecule fluorescent probes with large Stokes shifts for bioimaging. *Coord. Chem Rev.* 2023;489:215193. doi:10.1016/j.ccr.2023.215193
62. Gurubasavaraj PM, Sajjan VP, Muñoz-Flores BM, Jiménez Pérez VM, Hosmane NS. Recent advances in BODIPY compounds: synthetic methods, optical and nonlinear optical properties, and their medical applications. *Molecules.* 2022;27(6):1877. doi:10.3390/molecules27061877
63. Iliina K, MacCuaig WM, Laramie M, Jeouty JN, McNally LR, Henary M. Squaraine dyes: molecular design for different applications and remaining challenges. *Bioconjugate Chem.* 2019;31(2):194–213. doi:10.1021/acs.bioconjchem.9b00482
64. Rajasekar M. Recent Trends in Rhodamine derivatives as fluorescent probes for biomaterial applications. *J Mol Struct.* 2021;1235:130232. doi:10.1016/j.molstruc.2021.130232
65. Guria S, Ghosh A, Upadhyay P, et al. Small-molecule probe for sensing serum albumin with consequential self-assembly as a fluorescent organic nanoparticle for bioimaging and drug-delivery applications. *ACS Appl Bio Mater.* 2020;3(5):3099–3113. doi:10.1021/acsabm.0c00146
66. Zhang Y, Zhang G, Zeng Z, Pu K. Activatable molecular probes for fluorescence-guided surgery, endoscopy and tissue biopsy. *Chem Soc Rev.* 2022;51(2):566–593. doi:10.1039/d1cs00525a
67. Duan Q-J, Zhao Z-Y, Zhang Y-J, et al. Activatable fluorescent probes for real-time imaging-guided tumor therapy. *Adv. Drug Delivery Rev.* 2023. 114793. doi:10.1016/j.addr.2023.114793
68. Niu H, Liu J, O'Connor HM, Gunnlaugsson T, James TD, Zhang H. Photoinduced electron transfer (PeT) based fluorescent probes for cellular imaging and disease therapy. *Chem Soc Rev.* 2023;52(7):2322–2357. doi:10.1039/D1CS01097B
69. Zhu C, Kwok RT, Lam JW, Tang BZ. Aggregation-induced emission: a trailblazing journey to the field of biomedicine. *ACS Appl Bio Mater.* 2018;1(6):1768–1786. doi:10.1021/acsabm.8b00600
70. Huang Z, Li Q, Xue H, et al. Synthesis of an aggregation-induced emission (AIE) dye with pH-sensitivity based on tetraphenylethylene-pyridine for fluorescent nanoparticles and its applications in bioimaging and in vitro anti-tumor effect. *Colloids Surf B Biointerfaces.* 2024;234:113750. doi:10.1016/j.colsurfb.2024.113750
71. Wang DP, Zheng J, Jiang FY, et al. Facile and green fabrication of tumor- and mitochondria-targeted AIEgen-protein nanoparticles for imaging-guided photodynamic cancer therapy. *Acta Biomater.* 2023;168:551–564. doi:10.1016/j.actbio.2023.06.048
72. Luengo Morato Y, Ovejero Paredes K, Lozano Chamizo L, Marciello M, Filice M. Recent advances in multimodal molecular imaging of cancer mediated by hybrid magnetic nanoparticles. *Polymers.* 2021;13(17):2989. doi:10.3390/polym13172989
73. Ghosh T, Nandi S, Girigoswami A, et al. Carbon dots for multiuse platform: intracellular pH sensing and complementary intensified T1–T2 dual imaging contrast nanoprobe. *ACS Biomater Sci Eng.* 2024;10(2):1112–1127. doi:10.1021/acsbiomaterials.3c01389
74. Zhao W, He Z, Tang BZ. Room-temperature phosphorescence from organic aggregates. *Nature Rev Mater.* 2020;5(12):869–885. doi:10.1038/s41578-020-0223-z
75. Fang M, Yang J, Li Z. Light emission of organic luminogens: generation, mechanism and application. *Pro Mater Sci.* 2022;125:100914. doi:10.1016/j.pmatsci.2021.100914
76. Alzola-Aldamizetxebarria S, Fernández-Méndez L, Padro D, Ruiz-Cabello J, Ramos-Cabrer P. A comprehensive introduction to magnetic resonance imaging relaxometry and contrast agents. *ACS omega.* 2022;7(42):36905–36917. doi:10.1021/acsomega.2c03549
77. Wamelink IJ, Azizova A, Booth TC, et al. Brain Tumor Imaging without Gadolinium-based Contrast Agents: feasible or Fantasy? *Radiology.* 2024;310(2):e230793. doi:10.1148/radiol.230793
78. Choi JW, Moon W-J. Gadolinium deposition in the brain: current updates. *Korean j radiol.* 2019;20(1):134. doi:10.3348/kjr.2018.0356
79. Mathur M, Jones JR, Weinreb JC. Gadolinium deposition and nephrogenic systemic fibrosis: a radiologist's primer. *Radiographics.* 2020;40(1):153–162. doi:10.1148/rg.2020190110
80. Ndiaye D, Sy M, Pallier A, et al. Unprecedented kinetic inertness for a Mn²⁺-bispidine chelate: a novel structural entry for Mn²⁺-based imaging agents. *Angew Chem Int Ed.* 2020;59(29):11958–11963. doi:10.1002/anie.202003685
81. Gale EM, Wey H-Y, Ramsay I, Yen Y-F, Sosnovik DE, Caravan P. A manganese-based alternative to gadolinium: contrast-enhanced MR angiography, excretion, pharmacokinetics, and metabolism. *Radiology.* 2018;286(3):865–872. doi:10.1148/radiol.2017170977
82. Gholipour N, Akhlaghi M, Mokhtari Kheirabadi A, Geramifar P, Beiki D. Development of Ga-68 labeled, biotinylated thiosemicarbazone dextran-coated iron oxide nanoparticles as multimodal PET/MRI probe. *Int J Biol Macromol.* 2020;148:932–941. doi:10.1016/j.ijbiomac.2020.01.208
83. Qi G, Shi G, Wang S, et al. A novel pH-responsive iron oxide core-shell magnetic mesoporous silica nanoparticle (M-MSN) system encapsulating doxorubicin (DOX) and Glucose Oxidase (Gox) for pancreatic cancer treatment. *Int j Nanomed.* 2023. 7133–7147. doi:10.2147/IJN.S436253
84. Yang C, Che X, Zhang Y, et al. Hybrid FeWO₄-Hyaluronic acid nanoparticles as a targeted nanotheranostic agent for multimodal imaging-guided tumor photothermal therapy. *Int j Nanomed.* 2023;Volume 18:8023–8037. doi:10.2147/IJN.S432533
85. Wang P, Sun S, Bai G, Zhang R, Liang F, Zhang Y. Nanosized Prussian blue and its analogs for bioimaging and cancer theranostics. *Acta Biomater.* 2024.
86. Wang Y, Williams GR, Zheng Y, et al. Polydopamine-cloaked Fe-based metal organic frameworks enable synergistic multidimensional treatment of osteosarcoma. *J Colloid Interface Sci.* 2023;651:76–92. doi:10.1016/j.jcis.2023.07.146

87. Hu H, Zhang Y, Shukla S, Gu Y, Yu X, Steinmetz NF. Dysprosium-modified tobacco mosaic virus nanoparticles for ultra-high-field magnetic resonance and near-infrared fluorescence imaging of prostate cancer. *ACS nano*. 2017;11(9):9249–9258. doi:10.1021/acsnano.7b04472
88. Consolino L, Anemone A, Capozza M, et al. Non-invasive investigation of tumor metabolism and acidosis by MRI-CEST imaging. *Front Oncol*. 2020;10:161. doi:10.3389/fonc.2020.00161
89. Karan S, Cho MY, Lee H, et al. Hypoxia-responsive luminescent CEST MRI agent for in vitro and in vivo tumor detection and imaging. *J Med Chem*. 2022;65(10):7106–7117. doi:10.1021/acs.jmedchem.1c01745
90. Lindeman LR, Randtke EA, High RA, Jones KM, Howison CM, Pagel MD. A comparison of exogenous and endogenous CEST MRI methods for evaluating in vivo pH. *Magnetic Resonance Med*. 2018;79(5):2766–2772. doi:10.1002/mrm.26924
91. Jouclas R, Laine S, Eliseeva SV, et al. Lanthanide-based probes for imaging detection of enzyme Activities by NIR Luminescence, T1-and ParaCEST MRI. *Angew Chem*. 2024;136(16):e202317728. doi:10.1002/ange.202317728
92. Di Gregorio E, Papi C, Conti L, et al. A magnetic resonance imaging-chemical exchange saturation transfer (MRI-CEST) method for the detection of water cycling across cellular membranes. *Angew Chem*. 2024;136(6):e202313485. doi:10.1002/ange.202313485
93. Kombala CJ, Kotrotsou A, Schuler FW, et al. Development of a nanoscale chemical exchange saturation transfer magnetic resonance imaging contrast agent that measures pH. *ACS nano*. 2021;15(12):20678–20688. doi:10.1021/acsnano.1c10107
94. Köse G, Darguzyte M, Kiessling F. Molecular ultrasound imaging. *Nanomaterials*. 2020;10(10):1935. doi:10.3390/nano10101935
95. Luo Y, Fan C, Song Y, Xu T, Zhang X. Ultra-trace enriching biosensing in nanoliter sample. *Biosens Bioelectron*. 2022;210:114297. doi:10.1016/j.bios.2022.114297
96. Ling W, Nie J, Zhang D, et al. Role of contrast-enhanced ultrasound (CEUS) in the diagnosis of cervical lymph node metastasis in nasopharyngeal carcinoma (NPC) patients. *Front Oncol*. 2020;10:972. doi:10.3389/fonc.2020.00972
97. Challenging paradigms in tumour drug delivery. *Nat Mater*. 2020;19(5):477. doi:10.1038/s41563-020-0676-x
98. Zeng F, Du M, Chen Z. Nanosized contrast agents in ultrasound molecular imaging. *Front Bioeng Biotechnol*. 2021;9:758084. doi:10.3389/fbioe.2021.758084
99. Abou-Elkacem L, Bachawal SV, Willmann JK. Ultrasound molecular imaging: moving toward clinical translation. *Eur J Radiol*. 2015;84(9):1685–1693. doi:10.1016/j.ejrad.2015.03.016
100. Hao Y, Luo J, Wang Y, Li Z, Wang X, Yan F. Ultrasound molecular imaging of p32 protein translocation for evaluation of tumor metastasis. *Biomaterials*. 2023;293:121974. doi:10.1016/j.biomaterials.2022.121974
101. Feng Y, Hao Y, Wang Y, et al. Ultrasound molecular imaging of bladder cancer via extradomain b fibronectin-targeted biosynthetic GVs. *Int J Nanomed*. 2023;18:4871–4884. doi:10.2147/ijn.S412422
102. Yang H, Cai W, Lv W, et al. A new strategy for accurate targeted diagnosis and treatment of cutaneous malignant melanoma: dual-mode phase-change lipid nanodroplets as ultrasound contrast agents. *Int J Nanomed*. 2019;14:7079–7093. doi:10.2147/ijn.S207419
103. Ai C, Sun X, Xiao S, et al. CAFs targeted ultrasound-responsive nanodroplets loaded V9302 and GLULsiRNA to inhibit melanoma growth via glutamine metabolic reprogramming and tumor microenvironment remodeling. *J Nanobiotechnol*. 2023;21(1):214. doi:10.1186/s12951-023-01979-z
104. Liu R, Shi D, Guo L, et al. Ultrasound-targeted microbubble disruption with key nanodroplets for effective ferroptosis in triple-negative breast cancer using animal model. *Int J Nanomed*. 2023;18:2037–2052. doi:10.2147/ijn.S400495
105. Liao M, Du J, Chen L, et al. Sono-activated materials for enhancing focused ultrasound ablation: design and application in biomedicine. *Acta Biomater*. 2024;173:36–50. doi:10.1016/j.actbio.2023.11.004
106. Pellow C, Jafari Sojahrood A, Zhao X, Kolios MC, Exner AA, Goertz DE. Synchronous intravital imaging and cavitation monitoring of antivascular focused ultrasound in tumor microvasculature using monodisperse low boiling point nanodroplets. *ACS Nano*. 2024;18(1):410–427. doi:10.1021/acsnano.3c07711
107. Wang Q, He J, Qi Y, Ye Y, Ye J, Zhou M. Ultrasound-enhanced nano catalyst with ferroptosis-apoptosis combined anticancer strategy for metastatic uveal melanoma. *Biomaterials*. 2024;305:122458. doi:10.1016/j.biomaterials.2023.122458
108. Yang X, Zhao M, Wu Z, et al. Nano-ultrasonic contrast agent for chemoimmunotherapy of breast cancer by immune metabolism reprogramming and tumor autophagy. *ACS nano*. 2022;16(2):3417–3431. doi:10.1021/acsnano.2c00462
109. Qiu Y, Wu Z, Chen Y, et al. Nano ultrasound contrast agent for synergistic chemo-photothermal therapy and enhanced immunotherapy against liver cancer and metastasis. *Adv. Sci*. 2023;10(21):2300878. doi:10.1002/advs.202300878
110. Sridharan B, Lim HG. Advances in photoacoustic imaging aided by nano contrast agents: special focus on role of lymphatic system imaging for cancer theranostics. *J Nanobiotechnol*. 2023;21(1):437. doi:10.1186/s12951-023-02192-8
111. Zhao Z, Swartzchick CB, Chan J. Targeted contrast agents and activatable probes for photoacoustic imaging of cancer. *Chem Soc Rev*. 2022;51(3):829–868. doi:10.1039/d0cs00771d
112. Kesharwani P, Ma R, Sang L, et al. Gold nanoparticles and gold nanorods in the landscape of cancer therapy. *Mol Cancer*. 2023;22(1):98. doi:10.1186/s12943-023-01798-8
113. Zhang R, Kiessling F, Lammers T, Pallares RM. Unraveling the seedless growth of gold nanostars through fractional factorial design. *J Phys Chem C*. 2022;126(43):18580–18585. doi:10.1021/acs.jpcc.2c06396
114. Zhang R, Thoröe-Boveleth S, Chigrin DN, Kiessling F, Lammers T, Pallares RM. Nanoscale engineering of gold nanostars for enhanced photoacoustic imaging. *J Nanobiotechnol*. 2024;22(1):115. doi:10.1186/s12951-024-02379-7
115. Kim M, VanderLaan D, Lee J, et al. Hyper-branched gold nanoconstructs for photoacoustic imaging in the near-infrared optical window. *Nano Lett*. 2023;23(20):9257–9265. doi:10.1021/acs.nanolett.3c02177
116. Xu Q, Li D, Zhou H, et al. MnO₂-coated porous Pt@CeO₂ core-shell nanostructures for photoacoustic imaging-guided tri-modal cancer therapy. *Nanoscale*. 2021;13(39):16499–16508. doi:10.1039/D1NR03246A
117. Li L, Chen H, Shi Y, Xing D. Human-body-temperature triggerable phase transition of W-VO₂@PEG nanoprobes with strong and switchable NIR-II absorption for deep and contrast-enhanced photoacoustic imaging. *ACS nano*. 2022;16(2):2066–2076. doi:10.1021/acsnano.1c07511
118. Alibasha A, Khan S, Chatterjee T, Ghosh M. Unleashing the power of porphyrin photosensitizers: illuminating breakthroughs in photodynamic therapy. *J Photochem Photobiol B Biol*. 2023;248:112796. doi:10.1016/j.jphotobiol.2023.112796

119. Liolios C, Koutsikou TS, Salvanou EA, et al. Synthesis and in vitro proof-of-concept studies on bispecific iron oxide magnetic nanoparticles targeting PSMA and GRP receptors for PET/MR imaging of prostate cancer. *Int J Pharm.* 2022;624:122008. doi:10.1016/j.ijpharm.2022.122008
120. Wang P, Sun W, Guo J, et al. One pot synthesis of zwitterionic 99mTc doped ultrasmall iron oxide nanoparticles for SPECT/T1-weighted MR dual-modality tumor imaging. *Colloids Surf B Biointerfaces.* 2021;197:111403. doi:10.1016/j.colsurfb.2020.111403
121. Chen K, Li ZB, Wang H, Cai W, Chen X. Dual-modality optical and positron emission tomography imaging of vascular endothelial growth factor receptor on tumor vasculature using quantum dots. *Eur J Nucl Med Mol Imaging.* 2008;35(12):2235–2244. doi:10.1007/s00259-008-0860-8
122. Deng H, Konopka CJ, Prabhu S, et al. Dextran-mimetic quantum dots for multimodal macrophage imaging in vivo, ex vivo, and in situ. *ACS nano.* 2022;16(2):1999–2012. doi:10.1021/acsnano.1c07010
123. Ariztia J, Solmont K, Moise NP, et al. PET/fluorescence imaging: an overview of the chemical strategies to build dual imaging tools. *Bioconjugate Chem.* 2022;33(1):24–52. doi:10.1021/acs.bioconjchem.1c00503
124. Shi X, Xu P, Cao C, Cheng Z, Tian J, Hu X. PET/NIR-II fluorescence imaging and image-guided surgery of glioblastoma using a folate receptor α -targeted dual-modal nanoprobe. *Eur J Nucl Med Mol Imaging.* 2022;49(13):4325–4337. doi:10.1007/s00259-022-05890-x
125. Chen X, Zhou H, Li X, et al. Plectin-1 targeted dual-modality nanoparticles for pancreatic cancer imaging. *EBioMedicine.* 2018;30:129–137. doi:10.1016/j.ebiom.2018.03.008
126. Pan Y, Chen W, Yang J, Zheng J, Yang M, Yi C. Facile synthesis of gadolinium chelate-conjugated polymer nanoparticles for fluorescence/magnetic resonance dual-modal imaging. *Anal Chem.* 2018;90(3):1992–2000. doi:10.1021/acs.analchem.7b04078
127. Fu X, Fu S, Cai Z, et al. Manganese porphyrin/ICG nanoparticles as magnetic resonance/fluorescent dual-mode probes for imaging of sentinel lymph node metastasis. *J Mater Chem B.* 2022;10(48):10065–10074. doi:10.1039/d2tb01885c
128. Ding L, Lyu Z, Perles-Barbacaru TA, et al. Modular self-assembling dendrimer nanosystems for magnetic resonance and multimodality imaging of tumors. *Adv Mater.* 2023;36(7):e2308262. doi:10.1002/adma.202308262
129. Zhang L, Liu Y, Huang H, et al. Multifunctional nanotheranostics for near infrared optical imaging-guided treatment of brain tumors. *Adv Drug Deliv Rev.* 2022;190:114536. doi:10.1016/j.addr.2022.114536
130. Guo B, Feng Z, Hu D, et al. Precise deciphering of brain vasculatures and microscopic tumors with dual NIR-II fluorescence and photoacoustic imaging. *Adv Mater.* 2019;31(30):e1902504. doi:10.1002/adma.201902504
131. Cheng MHY, Harmatys KM, Charron DM, Chen J, Zheng G. Stable J-Aggregation of an aza-BODIPY-lipid in a liposome for optical cancer Imaging. *Angew Chem Int Ed Engl.* 2019;58(38):13394–13399. doi:10.1002/anie.201907754
132. Xu R, Jiao D, Long Q, et al. Highly bright aggregation-induced emission nanodots for precise photoacoustic/NIR-II fluorescence imaging-guided resection of neuroendocrine neoplasms and sentinel lymph nodes. *Biomaterials.* 2022;289:121780. doi:10.1016/j.biomaterials.2022.121780
133. Li S, Jiang W, Yuan Y, et al. Delicately designed cancer cell membrane-camouflaged nanoparticles for targeted (19)F MR/PA/FL imaging-guided photothermal therapy. *ACS Appl Mater Interf.* 2020;12(51):57290–57301. doi:10.1021/acsmami.0c13865
134. Huang M, Qi M, Yang H, et al. Noninvasive strategies for the treatment of tiny liver cancer: integrating photothermal therapy and multimodality imaging epcam-guided nanoparticles. *ACS Appl Mater Interf.* 2023;15(18):21843–21853. doi:10.1021/acsmami.3c00211
135. Baghy K, Ladányi A, Reszegi A, Kovalszky I. Insights into the tumor microenvironment-components, functions and therapeutics. *Int J Mol Sci.* 2023;24(24):17536. doi:10.3390/ijms242417536
136. Berrell N, Sadeghirad H, Blick T, et al. Metabolomics at the tumor microenvironment interface: decoding cellular conversations. *Med Res Rev.* 2024;44(3):1121–1146. doi:10.1002/med.22010
137. Li Y, Chen Q, Pan X, Lu W, Zhang J. New insight into the application of fluorescence platforms in tumor diagnosis: from chemical basis to clinical application. *Med Res Rev.* 2023;43(3):570–613. doi:10.1002/med.21932
138. Zhu W, Li X, Zheng G, et al. Preclinical and pilot clinical evaluation of a small-molecule carbonic anhydrase IX targeting PET tracer in clear cell renal cell carcinoma. *Eur J Nucl Med Mol Imaging.* 2023;50(10):3116–3125. doi:10.1007/s00259-023-06248-7
139. Li H, Feng Y, Luo Q, et al. Stimuli-activatable nanomedicine meets cancer theranostics. *Theranostics.* 2023;13(15):5386–5417. doi:10.7150/thno.87854
140. Sun R, Ma W, Ling M, et al. pH-activated nanoplatform for visualized photodynamic and ferroptosis synergistic therapy of tumors. *J Control Release.* 2022;350:525–537. doi:10.1016/j.jconrel.2022.08.050
141. Ghaemi B, Javad Hajipour M. Tumor acidic environment directs nanoparticle impacts on cancer cells. *J Colloid Interface Sci.* 2023;634:684–692. doi:10.1016/j.jcis.2022.12.019
142. Li Z, Li T, Zhang C, et al. A multispectral photoacoustic tracking strategy for wide-field and real-time monitoring of macrophages in inflammation. *Anal Chem.* 2021;93(24):8467–8475. doi:10.1021/acs.analchem.1c00690
143. Luo X, Hu D, Gao D, et al. Metabolizable near-infrared-ii nanoprobe for dynamic imaging of deep-seated tumor-associated macrophages in pancreatic cancer. *ACS Nano.* 2021;15(6):10010–10024. doi:10.1021/acsnano.1c01608
144. Erreni M, D'Autilia F, Avigni R, et al. Size-advantage of monovalent nanobodies against the macrophage mannose receptor for deep tumor penetration and tumor-associated macrophage targeting. *Theranostics.* 2023;13(1):355–373. doi:10.7150/thno.77560
145. Chong L, Jiang YW, Wang D, Chang P, Xu K, Li J. Targeting and repolarizing M2-like tumor-associated macrophage-mediated MR imaging and tumor immunotherapy by biomimetic nanoparticles. *J Nanobiotechnol.* 2023;21(1):401. doi:10.1186/s12951-023-02122-8
146. Hu Z, Fang C, Li B, et al. First-in-human liver-tumour surgery guided by multispectral fluorescence imaging in the visible and near-infrared-I/II windows. *Nat Biomed Eng.* 2020;4(3):259–271. doi:10.1038/s41551-019-0494-0
147. Xu H, Yuan L, Shi Q, Tian Y, Hu F. Ultrabright NIR-II nanoprobe for image-guided accurate resection of tiny metastatic lesions. *Nano Lett.* 2024;24(4):1367–1375. doi:10.1021/acs.nanolett.3c04483
148. Yu Q, Huang S, Wu Z, Zheng J, Chen X, Nie L. Label-free visualization of early cancer hepatic micrometastasis and intraoperative image-guided surgery by photoacoustic imaging. *J Nucl Med.* 2020;61(7):1079–1085. doi:10.2967/jnumed.119.233155
149. Liu JJ, Wang Z, Nie LM, et al. RGD-functionalised melanin nanoparticles for intraoperative photoacoustic imaging-guided breast cancer surgery. *Eur J Nucl Med Mol Imaging.* 2022;49(3):847–860. doi:10.1007/s00259-021-05545-3

150. Viana Cabral F, Quilez Albuquerque J, Roberts HJ, Hasan T. Shedding light on chemoresistance: the perspective of photodynamic therapy in cancer management. *Int J Mol Sci.* 2024;25(7):3811. doi:10.3390/ijms25073811
151. Feng S, Xiao Y, Lu J, et al. Tumor microenvironment sensitization via dual-catalysis of carbon-based nanoenzyme for enhanced photodynamic therapy. *J Colloid Interface Sci.* 2024;663:577–590. doi:10.1016/j.jcis.2024.02.160
152. Wang J, Sun J, Hu W, et al. A Porous Au@Rh Bimetallic Core-Shell Nanostructure as an H₂O₂-Driven Oxygenerator to Alleviate Tumor Hypoxia for Simultaneous bimodal imaging and enhanced photodynamic therapy. *Adv Mater.* 2020;32(22):e2001862. doi:10.1002/adma.202001862
153. Zhang L, Li CX, Wan SS, Zhang XZ. Nanocatalyst-mediated chemodynamic tumor therapy. *Adv Healthc Mater.* 2022;11(2):e2101971. doi:10.1002/adhm.202101971
154. Wu F, Zhang Q, Zhang M, et al. Hollow porous carbon coated FeS₂-based nanocatalysts for multimodal imaging-guided photothermal, starvation, and triple-enhanced chemodynamic therapy of cancer. *ACS Appl Mater Interf.* 2020;12(9):10142–10155. doi:10.1021/acsami.0c00170
155. Nie X, Xia L, Wang HL, et al. Photothermal therapy nanomaterials boosting transformation of Fe(III) into Fe(II) in tumor cells for highly improving chemodynamic therapy. *ACS Appl Mater Interf.* 2019;11(35):31735–31742. doi:10.1021/acsami.9b11291
156. He T, Yuan Y, Jiang C, et al. Light-triggered transformable ferrous ion delivery system for photothermal primed chemodynamic therapy. *Angew Chem Int Ed Engl.* 2021;60(11):6047–6054. doi:10.1002/anie.202015379
157. Yang L, Lu M, Wu Y, et al. Target design of multinary metal-organic frameworks for near-infrared imaging and chemodynamic therapy. *J Am Chem Soc.* 2023;145(48):26169–26178. doi:10.1021/jacs.3c08611
158. Zheng Z, Dai R, Jia Z, et al. Biodegradable multifunctional nanotheranostic based on Ag₂S-doped hollow BSA-SiO₂ for enhancing ROS-feedback synergistic antitumor therapy. *ACS Appl Mater Interf.* 2020;12(49):54356–54366. doi:10.1021/acsami.0c14855
159. An G, Zheng H, Guo L, et al. A metal-organic framework (MOF) built on surface-modified Cu nanoparticles eliminates tumors via multiple cascading synergistic therapeutic effects. *J Colloid Interface Sci.* 2024;662:298–312. doi:10.1016/j.jcis.2024.02.055
160. Cheng M, Kong Q, Tian Q, et al. Osteosarcoma-targeted Cu and Ce based oxide nanoplatfrom for NIR II fluorescence/magnetic resonance dual-mode imaging and ros cascade amplification along with immunotherapy. *J Nanobiotechn.* 2024;22(1):151. doi:10.1186/s12951-024-02400-z
161. Mirza Z, Karim S. Nanoparticles-based drug delivery and gene therapy for breast cancer: recent advancements and future challenges. *Elsevier.* 2021;69:226–237.
162. Qin W, Yang Q, Zhu C, et al. A distinctive insight into inorganic sonosensitizers: design principles and application domains. *Small.* 2024;20:2311228. doi:10.1002/sml.202311228
163. Wang T, Xu X, Zhang K. Nanotechnology-enabled chemodynamic therapy and immunotherapy. *Curr Cancer Drug Targets.* 2021;21(7):545–557. doi:10.2174/1568009621666210219101552
164. Xiang D, Zhou L, Yang R, et al. Advances in ferroptosis-inducing agents by targeted delivery system in cancer therapy. *Int j Nanomed.* 2024. 2091–2112. doi:10.2147/IJN.S448715

International Journal of Nanomedicine

Dovepress

Publish your work in this journal

The International Journal of Nanomedicine is an international, peer-reviewed journal focusing on the application of nanotechnology in diagnostics, therapeutics, and drug delivery systems throughout the biomedical field. This journal is indexed on PubMed Central, MedLine, CAS, SciSearch®, Current Contents®/Clinical Medicine, Journal Citation Reports/Science Edition, EMBase, Scopus and the Elsevier Bibliographic databases. The manuscript management system is completely online and includes a very quick and fair peer-review system, which is all easy to use. Visit <http://www.dovepress.com/testimonials.php> to read real quotes from published authors.

Submit your manuscript here: <https://www.dovepress.com/international-journal-of-nanomedicine-journal>